Journal of Pharmaceutical and Biomedical Analysis 280 (2026) 117602

Contents lists available at ScienceDirect

Journal of Pharmaceutical and Biomedical Analysis

journal homepage: www.journals.elsevier.com/journal-of-pharmaceutical-and-biomedical-analysis

UPLC-ESI-QToF-MS/MS profiling and anxiolytic-like effects of *Simira paraensis* (Baill.) Steyerm bark

Larissa Rodrigues Jales Martins [a,b], Nadia Eligia Nunes Pinto Paracampo [c], Paulo Riceli Vasconcelos Ribeiro [b], Francisco Oiram Filho [b], Amanda Maria Barros Alves [a], Hélcio Silva dos Santos [a,d], Jane Eire Silva Alencar de Menezes [a], Márcia Machado Marinho [a], Matheus Nunes da Rocha [a], Emmanuel Silva Marinho [a], Kirley Marques Canuto [a,b,*]

[a] *Programa de Pós-Graduação em Ciências Naturais, Universidade Estadual do Ceará, Av. Dr. Silas Munguba, 1700, Itaperi, Fortaleza,CE CEP 60714-903, Brazil*
[b] *Embrapa Agroindústria Tropical, R. Dra. Sara Mesquita, 2270, Pici, Fortaleza,CE CEP 60511-110, Brazil*
[c] *Embrapa Amazônia Oriental, R. Trav. Dr. Enéas Pinheiro, s/n°, Marco, Belém, PA CEP 66095-903, Brazil*
[d] *Curso de Química, Universidade Estadual Vale do Acaraú, R. Padre Francisco Sadoc, 850, Betânia, Sobral, CE CEP 62040-370, Brazil*

ARTICLE INFO

Keywords:
Rubiaceae
Simira paraensis
β-carboline alkaloids
Anxiety
Mass spectrometry

ABSTRACT

Simira paraensis (Baill.) Steyerm (Rubiaceae), popularly known as araribá-rosa, is a small tree found mainly in the Amazon. Studies on the genus *Simira* report a chemical composition rich in indole alkaloids of the *β*-carboline class, which are associated with effects on the central nervous system. The present study aimed to characterize the chemical profile and evaluate the anxiolytic activity of *S. paraensis* bark through *in vivo* and *in silico* assays. The powdered bark was extracted with a hydromethanolic solution, yielding a red-colored extract (SP-EMB), which was analyzed by Ultra High Performance Liquid Chromatography coupled to Electrospray Ionization Mass Spectrometry and Quadrupole-Time-of-Flight Analyzer (UPLC-ESI-QToF-MS/MS). The neuropharmacological activity was evaluated in zebrafish (*Danio rerio*) using locomotor activity, light/dark, novel tank, GABAergic neuromodulation, and PTZ-induced seizure **assays.** UPLC-ESI-QToF-MS/MS analysis revealed 15 *β*-carboline alkaloids, 4 phenolic acid derivatives, and 1 phenolic glycoside. Harmane, the major constituent, was isolated by preparative HPLC and identified by UPLC-ESI-QToF-MS/MS and NMR analyses. SP-EMB exhibited anxiolytic-like effects in both light/dark and novel tank tests, with low acute toxicity ($LD_{50} > 400$ mg·kg^{-1}) and reduced sedative effects compared to diazepam (DZP, 4 mg·kg^{-1}). Molecular docking showed that harmane and chlorogenic acid have high affinity for the $GABA_A$ receptor, indicating their influence on the anxiolytic effect. Both compounds showed low toxicity ($LD_{50} > 40$ mg·kg^{-1}) and dose-dependent anxiolytic-like activity without locomotor impairment. Furthermore, chlorogenic acid exhibited anxiolytic effects mediated by $GABA_A$ receptors. These findings may suggest that *S. paraensis* is a promising alternative source of anxiolytic agents with lower sedative effects.

1. Introduction

Rubiaceae is the fourth largest family of Angiosperms, with 132 genera and 1433 species, occurring predominantly in rainforests such as the Amazon. The classes of secondary metabolites found in it include iridoids, anthraquinones, terpenoids (diterpenes and triterpenes), indole alkaloids, flavonoids and other phenolic derivatives [1]. The genus *Simira* is characterized by the presence of *β*-carboline indole alkaloids [2], which are characterized by a tricyclic structure with two nitrogen atoms that varies according to the degree of saturation of the pyridinic ring.

β-carboline alkaloids exhibit diverse biological and pharmacological activities, especially in the central nervous system (CNS), and can act as anxiolytics, sedatives, anticonvulsants, or cause effects such as hallucinations and tremors, due to interaction with different receptors [3,4]. Anxiety, while a natural and adaptive response, may become pathological when excessive or persistent, as observed in anxiety disorders, including social anxiety disorder, which are characterized by a range of physical and emotional symptoms. Conventional pharmacological management relies primarily on benzodiazepines, such as diazepam

* Corresponding author at: Embrapa Agroindústria Tropical, R. Dra. Sara Mesquita, 2270, Pici, Fortaleza, CE CEP 60511-110, Brazil.
E-mail address: kirley.canuto@embrapa.br (K.M. Canuto).

https://doi.org/10.1016/j.jpba.2026.117602
Received 30 January 2026; Received in revised form 7 May 2026; Accepted 4 June 2026
Available online 5 June 2026

(DZP); however, their clinical use is often limited by adverse effects, including excessive sedation and the risk of tolerance and dependence [5]. In this context, increasing attention has been directed toward medicinal plants and herbal drugs as complementary or alternative strategies, particularly for the management of mild to moderate anxiety symptoms [6]. Within this framework, plants rich in bioactive secondary metabolites with known CNS activity have emerged as especially promising candidates for pharmacological investigation.

Simira paraensis (Baill.) Steyerm, popularly known as araribá-rosa, is a small tree endemic to the Amazon rainforest [7]. Although several studies have addressed the chemical composition and biological properties of the genus *Simira*, including antipyretic, purgative, and dye-related activities [2], investigations specifically focused on *S. paraensis* remain limited, with only a single report available to date [7]. This paucity of available data emphasizes the need for systematic chemical and pharmacological studies of this species.

Thus, the present study aimed to characterize the chemical profile of the crude methanolic extract obtained from *S. paraensis* bark using liquid chromatography coupled to mass spectrometry, to evaluate its anxiolytic activity in zebrafish experimental model, and to investigate its mechanism of action through molecular docking analyses.

2. Materials and methods

2.1. Plant material

The bark of *Simira paraensis* was collected in situ in the municipality of Belém (1° 26" 12.7′ S; 48° 26" 37.2′ W), in the State of Pará, in March 2024. The plant parts were separated, lyophilized, and stored in an ultrafreezer at −80 °C. This research was registered in the Brazilian System for the Management of Genetic Heritage and Associated Traditional Knowledge (SISGEN) under number A9E4150. A voucher specimen of *Simira paraensis* was authenticated by a botanist and deposited in the Herbarium IAN at Embrapa Amazônia Oriental under accession number IAN 202.907.

2.2. Solvents, drugs, and reagents

LC-MS grade solvents were purchased from Merck® (Darmstadt, Germany); ultrapure water (18.2 MΩ·cm at 25 °C) was obtained from a Milli-Q purification system (Millipore, Bedford, USA). Acetic acid PA (Synth®), sodium hydroxide PA (Dynamic®) and sodium sulfate (Dynamic®), diazepam (DZP, Neo Química®), dimethyl sulfoxide (3% DMSO, Dynamic®), flumazenil (FMZ, Sandoz®), pentylenetetrazol (PTZ, Sigma Aldrich®). Additionally, an analytical standard of chlorogenic acid (> 95%) was purchased from Sigma-Aldrich.

2.3. Extraction

The bark of *S. paraensis* (1.0 g) was extracted with methanol:water (90:10, v/v), previously acidified with acetic acid to pH 2.0. Maceration was carried out in an ultrasound bath (40 kHz, 25 ± 2 °C) for 30 min and repeated four times, followed by vacuum filtration. The filtrate obtained was neutralized to pH 7.0–7.5 with 10% NaOH solution and then concentrated in a rotary evaporator and dried under a nitrogen stream. The resulting extract, named Crude Methanol Extract (SP-EMB), was stored at −80 °C until subsequent analyses.

2.4. Chemical analyses

2.4.1. UPLC-ESI-QToF-MS/MS analysis

The SP-EMB (4 mg) was dissolved in 2 mL of methanol:water (50:50, v/v) and filtered through a PTFE membrane (0.22 μm). Analyses were performed on a Waters UPLC-ESI-QToF-MS/MS system. Chromatographic separation was performed on an Acquity BEH C18 column (150 × 2.1 mm, 1.7 μm), maintained at 50 °C. A 5 μL aliquot of SP-EMB was eluted with a mobile phase composed of deionized ater (A) and acetonitrile (B), both containing formic acid (0.1% v/v), in an exploratory gradient: 1–50% B (8 min), 98% B (8.1–12.0 min), 100% B (12.1–13.5 min), 1% B (13.6–15 min) and a flow rate of 0.5 mL·min^{-1}. Ionization was performed using an electrospray ionization source in positive and negative ESI modes, acquired in the range of 110–1180 Da, and the optimized instrumental parameters were: capillary voltage at 3.2 kV (positive), 2.8 kV (negative), cone voltage at 40 V, source temperature at 125 °C, desolvation temperature at 250 °C, and desolvation gas flow rate at 600 L·h^{-1}. The system was controlled using MassLynx 2.0 software (Waters Corporation). Compound characterization was based on molecular formulas generated by MassLynx 4.2 (error < 5 ppm), isotopic matching (i-fit), MS fragmentation patterns, and chemotaxonomic surveys for the genus *Simira* using the SciFinder database.

2.4.2. Isolation and identification of harmane

The alkaloid harmane was isolated by preparative high-performance liquid chromatography (prep-HPLC) using a system comprising a quaternary gradient pump (Waters 2555), UV–Vis detector (Waters 2489), and fraction collector (Waters Fraction Collector III). Separation was performed on a reverse-phase C18 column (SunFire Prep, 100 × 19 mm, 5 μm). The mobile phase consisted of ultrapure water (A) and methanol (B), both acidified with 0.05% trifluoroacetic acid, using a gradient elution program: 60% B (0 min), increased linearly to 100% B over 20 min, maintained until 25 min, and returned to 60% B at 30 min. The flow rate was 5 mL min^{-1}, with a total run time of 30 min at 25 °C. A fixed injection volume of 1 mL (20 mg extract) was used, and chromatograms were monitored at 352 nm. Fractions corresponding to the harmane peak (t_R = 9.13 min) were collected, pooled, and concentrated to yield the isolated compound. Preparative conditions were previously optimized on an analytical HPLC system (Shimadzu LC−20AB Prominence) fitted to an SPD-M20A diode array detector (DAD) and a C18 column (Shim-pack CLC–ODS (M), 150 × 4.6 mm, 5 μm). Chromatographic purity was assessed by HPLC-DAD using area normalization at 352 nm, while peak purity was evaluated by comparing UV spectra at the upslope, apex, and downslope of the peak.

The identification of the isolated compound was confirmed by UPLC-ESI-QToF-MS/MS and nuclear magnetic resonance (NMR) spectroscopy. One- and two-dimensional NMR spectra (COSY, HSQC, and HMBC) were recorded on a Bruker Neo spectrometer operating at 600 MHz for ^{1}H and 150 MHz for $^{1\ 3}$C, equipped with a 5 mm inverse-detection One Probe BBFO and a z-axis field gradient. The sample was dissolved in MeOD and its spectroscopic data were compared with literature values. Afterwards, this purified compound was used for the biological assays.

2.5. Studies in animal models

2.5.1. Zebrafish

Zebrafish (*Danio rerio*) (aged 90–120 days; 0.4 ± 0.1 g, 3.5 ± 0.5 cm), wild, of both sexes, were acquired from a local store (Fortaleza, Ceará, Brazil). The animals were kept in a 10 L glass aquarium (30 × 15 × 20 cm) (n = 3/L), circadian cycle of 14–10 h (light/dark) with chlorinated water (ProtecPlus®) and air pump with submersible filters, under a temperature of 25 °C and pH 7.0. The fish received food (Spirulina®) ad libitum 24 h before the experiments. Before drug administration, the animals were anesthetized in ice water, and after the experiments, the animals were sacrificed by immersion in ice water (2 and 4 °C) for 1 min until loss of opercular movement. The work was approved by the Ethics Committee on the Use of Animals of the State University of Ceará (CEUA-UECE; No. 04983945/2021) in accordance with the Ethical Principles of Animal Experimentation.

2.5.2. General protocol

Zebrafish of both sexes were randomly selected for the experiments, anesthetized in ice water, and transferred to a moist sponge. Animals

were treated with 20 μL of either the extract (40, 200, and 400 mg·kg^{-1}) or pure compounds (4, 20, and 40 mg·kg^{-1}) by oral administration, while DZP (4 mg·kg^{-1}) and 3% DMSO were used as positive and vehicle controls, respectively.

2.5.3. Toxicity test

Fish (n = 6 / group) were treated following the general protocol guidelines and left to rest for mortality rate analysis for a period of 96 h. The number of dead fish in each group was recorded every 24 h, and dead individuals were removed from the environment at each evaluation. The lethal dose capable of killing 50% of the animals (LD_{50}) was estimated using the Trimmed Spearman-Karber mathematical method with a 95% confidence interval.

2.5.4. Locomotor activity (Open Field Test)

The open field test was performed to assess the presence or absence of alterations in motor coordination in animals. The animals (n = 6/group) were pre-treated as described in the general protocol. DZP (4 mg·kg^{-1}) and 3% DMSO were used as positive and negative controls, respectively. After 60 min of treatment, the animals were individually placed in glass Petri dishes (10 × 15 cm with quadrants at the bottom of the dish), containing the same aquarium water. Locomotor activity was analyzed by counting the number of line crossings (CL), recorded during 0–5 min.

2.5.5. Anxiety-like behavior assays

2.5.5.1. Light/dark test. The experiment was conducted in a glass aquarium (30 cm × 15 cm × 20 cm) divided into a light area and a dark area. The aquarium was filled to 3 cm with dechlorinated tap water, simulating a new shallow environment different from a conventional aquarium and capable of inducing anxiety behaviors. The sample was administered to the animals (n = 6/group) as described in the general protocol. The negative and positive control groups consisted of 3% DMSO and 4 mg·kg^{-1} DZP solution, respectively. After 60 min, the animals were individually placed in the light zone and the anxiolytic effect was measured based on the time spent in the light zone of the aquarium within 5 min of observation [8].

2.5.5.2. New tank test. Fish from each experimental group, following a 30 min exposure to SP-EMB extract, DZP (4 mg·kg^{-1}), or 3% DMSO (control), were individually transferred to a rectangular tank (20 × 15 × 12 cm; total capacity 2.8 L). The lateral and rear walls of the tank were covered with white paper to minimize external visual stimuli, while the front wall remained uncovered to allow video recording. Behavioral activity was recorded immediately for 5 min. The tank was virtually divided into two equal horizontal zones (upper and lower; 6 cm each) to assess locomotor performance and anxiety-like behavior. The following parameters were quantified: total distance traveled, mean swimming speed, time spent and distance traveled in the upper zone, and percentage of exploration. Video recordings were analyzed using ToxTrack software, as previously described by Moreira and Luchiari (2022). [9]

2.5.6. Evaluation of GABAergic Neuromodulation

The GABAergic neuromodulation involved in the anxiolytic effect was performed through pretreatment with FMZ ($GABA_A$ antagonist) before the light/dark test [10]. Fish (n = 6/group) were pretreated with FMZ (4 mg·kg^{-1}; 20 μL; v.o.). After 15 min, the dose with the highest anxiolytic efficacy found in the previously performed test was administered. 3% DMSO (vehicle; 20 μL; v.o.) was used as a negative control and DZP (4 mg·kg^{-1}, 20 μL; v.o.) was used as a $GABA_A$ agonist. After 60 min of treatment, the animals underwent the light/dark test, as described previously.

2.5.7. Pentylenetetrazol (PTZ)-induced seizure

Animals were treated as described in the general protocol. After 30 min, animals were individually exposed by immersion in a 10 mM PTZ solution in a 250 mL beaker. Seizure behavior was analyzed by trained observers, measured in seconds, and classified according to stages: I - drastic increase in swimming activity; II - swirling behavior; III - clonus-like seizures, followed by loss of posture when the animal falls to its side and remains motionless for 1–3 s. At the end of the evaluation of the three stages of the test, the animals were euthanized on ice [8].

2.5.8. Statistical analysis

Results were expressed as mean values ± standard error of the mean for each group of 6 animals (n = 6). After confirming the normality of distribution and homogeneity of the data, the differences between the groups were subjected to analysis of variance - one-way ANOVA or Kruskal-Walles test, followed by *Tukey's* test. All analyses were performed using GraphPad Prism v. 8.0.1 software. The level of statistical significance was set at 5% ($p < 0.05$).

2.6. Molecular docking

Two-dimensional representations of the ligands were plotted and rendered using the academic license software MarvinSketch® Neon.3 LTS, Chemaxon© (https://chemaxon.com/marvin), for structural optimization by the Merck Molecular Force Field (MMFF94) method, using the Avogadro2 software (https://two.avogadro.cc/index.html), configured to perform 9000 calculation steps with a convergence limit of 10^{-6} units using the Steepest Descent algorithm [11], with a resolution of 3.58 Å.

The three-dimensional structure of the $GABA_A$ receptor was obtained from the RCSB Protein Data Bank (https://www.rcsb.org/) under PDB code 6HUP [12] at a resolution of 3.58 Å. Water molecules (H_2O) and the ligand DZP were removed, and Gasteiger charges were calculated after adding polar hydrogens. The grid box was defined to cover the entire conformational space of the protein, with dimensions x = 126, y = 102, and z = 127 (in Å) and centered at coordinates x = 125.25, y = 139.52, and z = 136.02, using the AutoDockTools software [13].

AutoDockVina (https://vina.scripps.edu/) was configured to run 50 independent cycles with 20 poses per cycle for each ligand, using the Lamarckian Genetic Algorithm (LGA) with an exhaustivity parameter of 64. The selection criterion for the best pose included a ligand-receptor complex with an affinity energy ≤ −6.0 kcal·mol^{-1} and a Root Mean Square Deviation (RMSD) ≤ 2.0 [14].

3. Results and discussion

3.1. Chemical characterization of SP-EMB

UPLC-ESI-QToF-MS/MS analysis allowed the chemical characterization of 20 compounds in SP-EMB, in both positive and negative ionization modes (Fig. 1). All compounds (Fig. 2) were identified according to molecular formulas, fragmentation patterns, and comparison with literature data (Table 1). The MS and MS/MS mass spectra of all substances (Figs. S1-S21) and the proposed fragmentation patterns of those belonging to the alkaloid class (Figs. S22-S26) are presented in the supplementary material.

Peaks **1** and **2** were assigned to phenolic glycosides. Peak **1** (tr = 1.87 min) showed precursor ion [M-H]$^-$ at m/z 433.1346 ($C_{18}H_{25}O_{12}$) and diagnostic ions at m/z 293 and 233 (Fig. S1), allowing its characterization as the canthoside C or D isomer **(1)**, previously reported in *Canthium berberidifolium* (Rubiaceae) [15]. Peak **2** (tr = 2.19 min) showed precursor ion [M-H]$^-$ at m/z 461.1295 ($C_{19}H_{25}O_{13}$) and diagnostic ions at m/z 167 and 123 (Fig. S2), which was characterized as hydroxy-methoxy-benzoic acid-*O*-pentosyl hexoside **(2)** [16].

Peaks **4**, **6** and **9** were assigned to phenylpropanoids, i.e., cinnamic

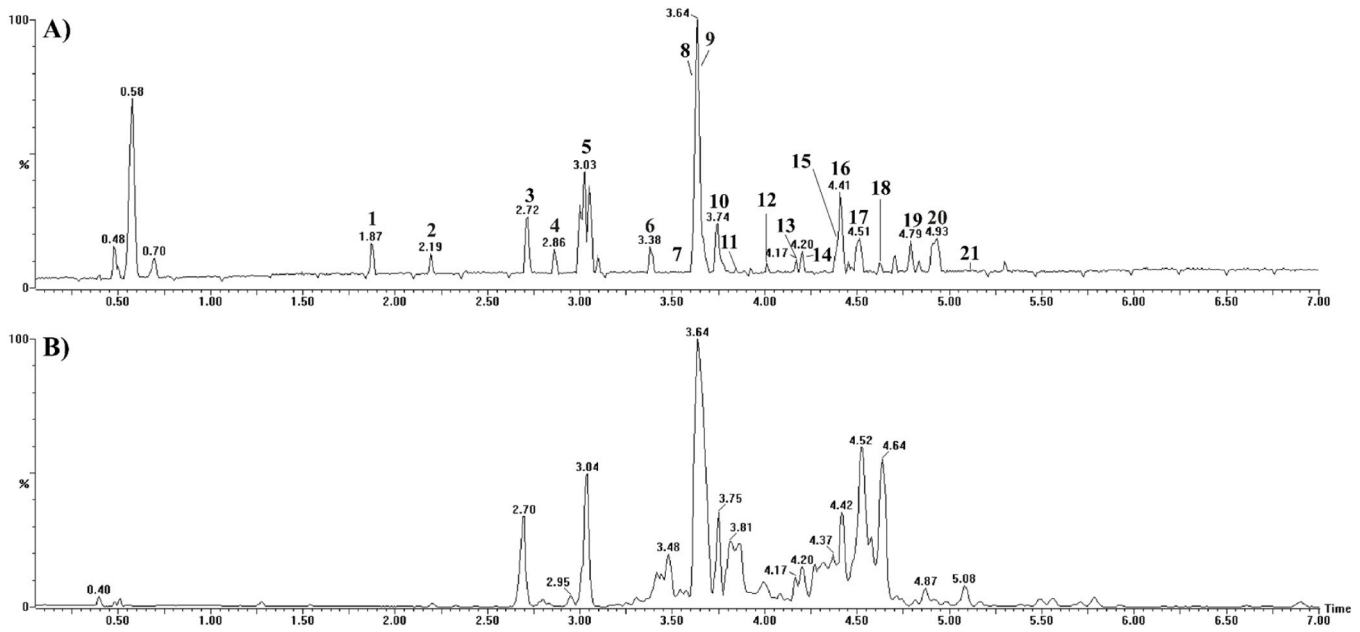

Fig. 1. Chromatogram of the methanolic extract of *Simira paraensis* stem bark by UPLC-ESI-QToF-MS/MS analyses in positive (A) and negative (B) ionization modes.

acid derivatives. Peak **4** (tr = 2.86 min) exhibited deprotonated precursor ion [M-H]$^-$ at m/z 353.0873 ($C_{16}H_{17}O_9$), as well as the fragment ion at m/z 191 (Fig. S4), which corresponds to the departure of deprotonated quinic acid ($C_7H_{12}O_6$), confirming the identification as chlorogenic acid **(4)** [17,18]. Peak **6** (tr = 3.38 min) exhibited a deprotonated precursor ion [M-H]$^-$ at m/z 337.0923 ($C_{16}H_{17}O_8$) and diagnostic ions at m/z 191 and 163 (Fig. S6). The fragmentation pattern is consistent with coumaroylquinic acid derivatives, particularly due to the presence of the diagnostic ions corresponding to deprotonated quinic acid ($C_7H_{12}O_6$, m/z 191) [17] and *p*-coumaric acid ($C_9H_8O_3$, m/z 163), supporting the annotation of this peak as 5-*O*-*p*-coumaroylquinic acid **(6)** [18]. Peak **9** (tr = 3.64 min) exhibited deprotonated precursor ion [M-H]$^-$ at m/z 367.1029 ($C_{17}H_{19}O_9$) and fragment ions at m/z 193, 191 and 173 (Fig. S9). These fragment ions were assigned to ferulic acid ($C_{10}H_{10}O_4$, m/z 193) and quinic acid ($C_7H_{12}O_6$, m/z 191) [17], while the ion at m/z 173 was attributed to the dehydration of quinic acid through the loss of H_2O (18 Da). Therefore, peak **9** was annotated as 3-*O*-feruloylquinic acid **(9)** [18].

Peaks **3**, **5**, **8**, **10**, **12** and **13** were assigned to alkaloid compounds. Peak **3** (tr = 2.70 min) and **5** (tr = 3.03 min) exhibited similar precursor ions [M + H]$^+$ at m/z 513.1877 and 513.1882 ($C_{26}H_{29}N_2O$). MS/MS yielded fragment ions with m/z 469, 351, 333, 307 (Figs. S3 and S5), which are part of the structure of an indolic-*β*-carboline alkaloid with a secologanin group [19]. According to the fragmentation proposal (Fig. S22), these peaks are justified by the exit of glucose ($C_6H_{10}O_5$, m/z 162) and carbon dioxide (CO_2, m/z 44), being identified as the isomers ophiorine A **(3)** and ophiorine B **(5)**. These compounds were previously described in several *Simira* species such as *S. glaziovii, S. tinctoria, S. williamsii* and *S. grazielae* [2,19–21]. Peak **8** (tr = 3.63 min) showed the highest intensity in the chromatogram, exhibiting a protonated precursor ion [M + H]$^+$ at m/z 183.0922 ($C_{12}H_{11}N_2$) and fragment ions m/z 168, 142 and 115 (Fig. S8) due to the departure of the methyl radical (Me$^\bullet$, m/z 15), the cyano radical (CN$^\bullet$, m/z 26) and, together, ethyne (C_2H_2, m/z 26) and the hydrogen ion (Fig. S23), being characterized as harmane **(8)** [22]. Furthermore, this compound was isolated by HPLC with a purity grade of 97% (Fig. S27). Its ^{1}H and ^{13}C NMR data (Figs. S28-S30) were consistent with the structure of the *β*-carboline alkaloid harmane. Signal assignments were established based on the combined analysis of 1D and 2D NMR spectra (Tab. S1), allowing unambiguous correlation between protons and carbons in the fused aromatic system. The spectroscopic data are in agreement with those reported in the literature for harmane [23]. Harmane is considered as a chemotaxonomic marker of the genus *Simira* [2].

Peak **10** (tr = 3.75 min) exhibited a protonated precursor ion [M + H]$^+$ at m/z 513.1873 ($C_{26}H_{29}N_2O_9$), similar to those observed for ophiorine A **(3)** and ophiorine B **(5)**, together with diagnostic fragment ions at m/z 469, 351, 307, and 183 (Fig. S10). Except for the ion at m/z 183, the remaining fragments were also detected in peaks **3** and **5** (Figs. S3 and S5), supporting similar fragmentation pathways involving the neutral losses of glucose ($C_6H_{10}O_5$, 162 Da) and carbon dioxide (CO_2, 44 Da), which account for the ions at m/z 351 and 307. However, the relative intensity of the ion at m/z 307 was lower in peak 10 (~63%) than in peaks 3 and 5 (100%), suggesting structural differences in the moiety bearing the carboxyl group [19]. Furthermore, the ion at m/z 183 indicates cleavage of the secologanin portion ($C_{14}H_{18}O_9$, 330 Da), yielding the characteristic *β*-carboline core. Based on the proposed fragmentation pathway (Fig. S24), peak **10** was identified as lyalosidic acid **(10)** [20]. This compound has been describer for *S. tinctoria, S. williamsii* and *S. grazielae* [2,20]. Peak **12** (tr = 3.99 min) showed the protonated precursor ion [M + H]$^+$ at m/z 517.2186 ($C_{26}H_{33}N_2O_9$), which was noted as strictosidinic acid **(12)** [19], since the fragments at m/z 500, 338 and 320 (Fig. S12) are justified by the departure of ammonia (NH_3, m/z 17), glucose ($C_6H_{10}O_5$, m/z 162) and water (H_2O, m/z 18) (Fig. S25), respectively. Furthermore, m/z 144 (Fig. S12) is indicative of a tetrahydro-*β*-carboline or dihydro-*β*-carboline indole skeleton. Peak **13** (tr = 4.17 min) showed the protonated precursor ion [M + H]$^+$ at m/z 531.2343 ($C_{27}H_{35}N_2O$), i.e., a mass 14 units greater than compound **12**, indicating that peak **13** corresponds to a structure with an ester function instead of a carboxylic acid (Fig. S26). In addition, it showed the same diagnostic ion as m/z 144 (Figs. S13 and S26), being identified as strictosidine **(13)**. Both **12** and **13** were previously found in *S. grazielae* [19].

Peaks **11** (tr = 3.81 min), **14** - **19** (tr = 4.20; 4,37; 4.42; 4.52; 4.64 and 4.87 min, respectively) and **21** (tr = 5.08 min) had ions at m/z 183 and 182, in positive mode (Fig. S11, S14-S19 and S21). The occurrence of these characteristic fragment ions, commonly associated with the core *β*-carboline scaffold, allowed their tentative classification as *β*-carboline alkaloid derivatives [24]. While peak **11** displayed the precursor ion [M + H]$^+$ at m/z 325.1552 ($C_{19}H_{21}N_2O_3$), peaks **14-19** showed the same protonated precursor ion at m/z 339.1709 ($C_{20}H_{23}N_2O_3$) and peak **21** at

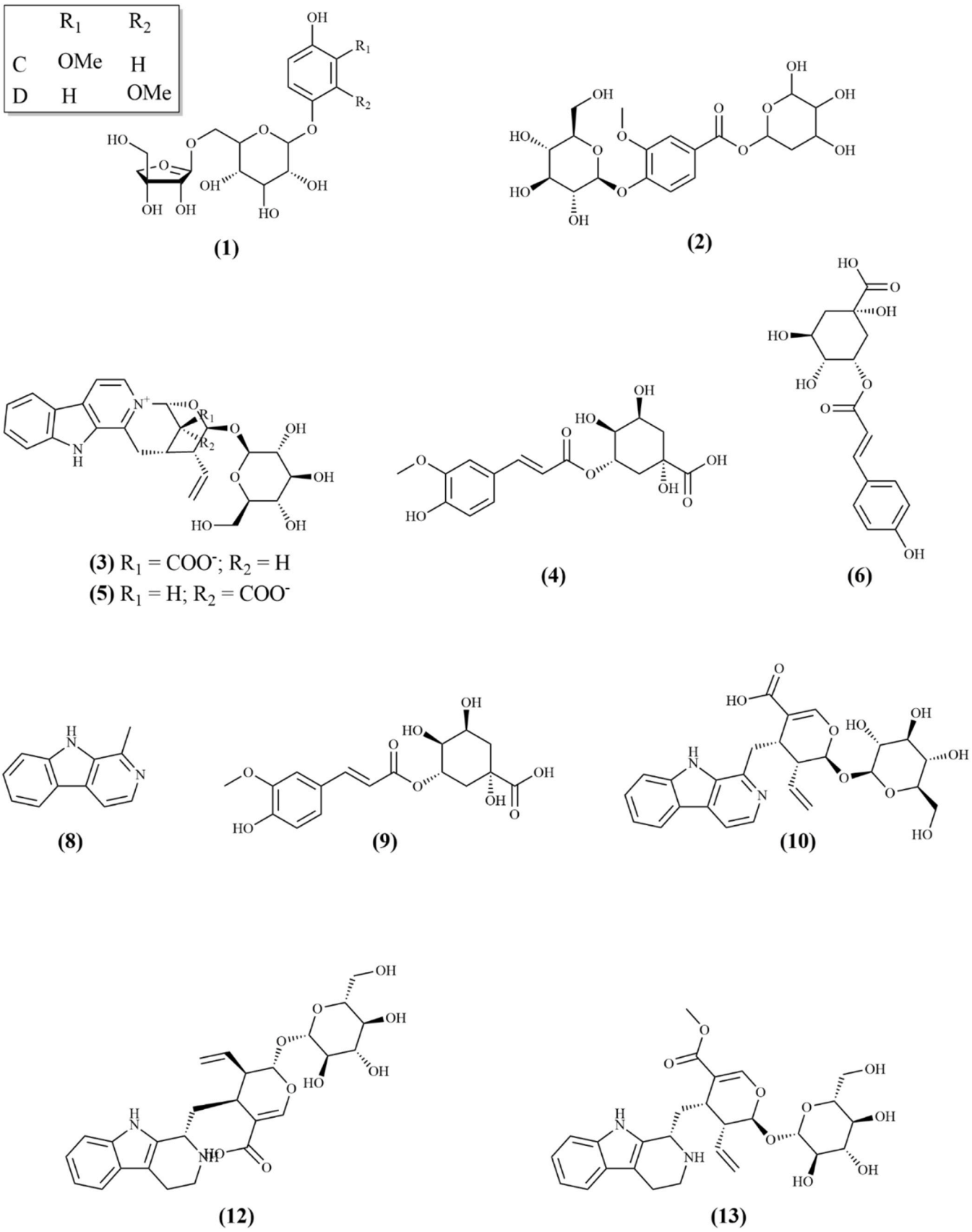

Fig. 2. Structure of substances tentatively identified in SP-EMB of *Simira paraensis* trunk bark using UPLC-QToF-MS/MS.

Table 1
Compounds tentatively identified in SP-EMB of *Simira paraensis* trunk bark using UPLC-QToF-MS/MS.

Peak	*RT* (min)	$[M - H]^-$/ $[M + H]^+$ Obs	$[M-H]^-$/ $[M + H]^+$ Calc.	MS^2 Fragments	Empirical formula	Error (ppm)	Tentative name	Ref.
1	1.87	433.1335/-	433.1346/-	293.0864, 233.0656	$C_{18}H_{25}O_{12}$	−2.5	Canthoside C or D	[15]
2	2.19	461.1298/-	461.1295/-	167.0340, 123.0441	$C_{19}H_{25}O_{13}$	0.7	Hydroxy-methoxy-benzoic acid-*O*-pentosyl hexoside	[16]
3	2.70	-/513.1877	-/513.1873	469.1978, 351.1352, 307.1453	$C_{26}H_{29}N_2O_9$	0.8	Ophiorine A	[19, 21]
4	2.86	353.0873/-	353.0873/-	191.0553	$C_{16}H_{17}O_9$	0.0	Chlorogenic acid	[18, 54]
5	3.03	-/513.1882	-/513.1873	469.1984, 351.1357, 333.1252, 307.1458	$C_{26}H_{29}N_2O_9$	1.8	Ophiorine B	[19, 21]
6	3.38	337.0922/-	337.0923/-	191.0550, 163.0392	$C_{16}H_{17}O_8$	−0.3	5-*O*-*p*-Coumaroylquinic acid	[18]
7	3.48	-/649.2612	-/649.2609	487.2086, 469.1983, 307.1457	$C_{31}H_{41}N_2O_{13}$	0.5	Unknown indole alkaloid	-
8	3.63	-/183.0925	-/183.0922	168.0690, 142.0643, 115.0543	$C_{12}H_{11}N_2$	1.6	Harmane	[22]
9	3.64	367.1026/-	367.1029/-	193.0503, 191.0550, 173.0444	$C_{17}H_{19}O_9$	−0.8	3-*O*-Feruloylquinic acid	[18]
10	3.75	-/513.1876	-/513.1873	469.1976, 351.1351, 307.1451, 183.0913	$C_{26}H_{29}N_2O_9$	0.6	Lyalosidic acid	[20]
11	3.81	-/325.1559	-/325.1552	183.0909, 182.0847	$C_{19}H_{21}N_2O_3$	2.2	*β*-carboline alkaloid type derivative	[24]
12	3.99	-/517.2192	-/517.2186	144.0813	$C_{26}H_{33}N_2O_9$	1.2	Strictosidinic acid	[19, 55]
13	4.17	-/531.2346	-/531.2343	326.1404, 308.1372, 183.0908, 182.0847, 144.0812	$C_{27}H_{35}N_2O_9$	0.6	Strictosidine	[19]
14	4.20	-/339.1713	-/339.1709	183.0904, 182.0843	$C_{20}H_{23}N_2O_3$	1.2	*β*-carboline alkaloid type derivative	[24]
15	4.37	-/339.1710	-/339.1709	183.0908, 182.0847	$C_{20}H_{23}N_2O_3$	0.3	*β*-carboline alkaloid type derivative	[24]
16	4.42	-/339.1711	-/339.1709	183.0908, 182.0846	$C_{20}H_{23}N_2O_3$	0.6	*β*-carboline alkaloid type derivative	[24]
17	4.52	-/339.1714	-/339.1709	183.0910, 182.0847	$C_{20}H_{23}N_2O_3$	1.5	*β*-carboline alkaloid type derivative	[24]
18	4.64	-/339.1715	-/339.1709	183.0911, 182.0846	$C_{20}H_{23}N_2O_3$	1.8	*β*-carboline alkaloid type derivative	[24]
19	4.87	-/353.1871	-/353.1865	183.0909, 182.0844	$C_{21}H_{25}N_2O_3$	1.7	*β*-carboline alkaloid type derivative	-
20	4.93	545.1658/-	545.1659/-	353.1022, 191.0553	$C_{27}H_{29}O_{12}$	−0.2	Unknown	-
21	5.08	-/371.2337	-/371.2335	307.1448, 183.0925, 182.0874, 144.0810	$C_{22}H_{31}N_2O_3$	0.5	*β*-carboline alkaloid type derivative	-

$[M + H]^+$ *m/z* 371.2335 ($C_{22}H_{31}N_2O_3$).

Peak 7 (*tr* = 3.48 min) exhibited a protonated precursor ion $[M + H]^+$ at *m/z* 649.2609 ($C_{31}H_{41}N_2O$) and was tentatively characterized as an unknown indole alkaloid due to the presence of diagnostic fragment ions at *m/z* 469 and 307 (Fig. S7), which were also observed for ophiorine A **(3)** and ophiorine B **(5)**. Peak **20** presented a precursor ion $[M-H]^-$ at *m/z* 545.1658 and MS/MS fragments at *m/z* 353 and 191, corresponding to molecular formula $C_{27}H_{29}O_{12}$, but remaining unidentified (Fig. S20).

Thus, the chemical profiling of *Simira paraensis* substantially expands the chemotaxonomic knowledge of the species, genus, and its botanical family. Among the identified compounds, canthoside C/D isomer **(1)**, chlorogenic acid **(4)**, 5-*O*-*p*-coumaroylquinic acid **(6)**, and 3-*O*-feruloylquinic acid **(9)** are herein reported for the first time in *S. paraensis*. In addition, hydroxy-methoxy-benzoic acid-*O*-pentosyl hexoside **(2)** represents the first report for the Rubiaceae family. Although ophiorine A **(3)**, ophiorine B **(5)**, harmane **(8)**, lyalosidic acid **(10)**, strictosidinic acid **(12)**, and strictosidine **(13)** have already been described in other *Simira* species, this is the first report of these alkaloids in *Simira paraensis*. Furthermore, the detection of several unidentified *β*-carboline derivatives (peaks 11 and 14–21) and an unknown indole alkaloid **(7)** highlights the remarkable alkaloidal diversity of the species and reinforces the potential of *S. paraensis* as a promising source of previously undescribed specialized metabolites.

3.2. Neuropharmacological evaluation of SP-EMB in zebrafish

The doses of SP-EMB tested (40, 200, and 400 $mg{\cdot}kg^{-1}$) did not induce toxicity in adult zebrafish throughout the 96 h observation period ($LD_{50} > 400\ mg{\cdot}kg^{-1}$), as evidenced by the absence of significant mortality and the lack of apparent anatomical alterations ($p > 0.05$). These findings confirm the suitability of these doses for subsequent *in vivo* pharmacological evaluations.

Locomotor activity was reduced at all tested doses when compared with the negative control (3% DMSO). However, this reduction was significantly less pronounced than that observed for DZP, indicating an intermediate sedative profile (Fig. 3A; ****$p < 0.0001$ vs. Control; ####$p < 0.0001$ vs. DZP). This behavioral pattern suggests that SP-EMB exerts moderate CNS depressant effects, consistent with compounds known to modulate zebrafish CNS activity [25].

Anxiolytic-like behavior was initially assessed using the light/dark test, a validated paradigm based on the innate preference of zebrafish for darker environments as an adaptive antipredatory response, analogous to rodents [26]. SP-EMB elicited a significant anxiolytic effect exclusively at the intermediate dose (200 $mg{\cdot}kg^{-1}$; *$p < 0.05$, ***$p < 0.001$ vs. Control), as demonstrated by an increased time spent in the illuminated compartment (Fig. 3B). Notably, this effect was comparable to that observed for DZP (4 $mg{\cdot}kg^{-1}$), the positive control, suggesting pharmacological relevance and supporting further investigation of its mechanism of action.

To further validate this anxiolytic-like profile through a complementary behavioral model, the novel tank test was performed, which evaluates anxiety-like responses based on vertical exploratory behavior. Upon introduction into a new environment, fish exhibit characteristic bottom-dwelling and freezing behavior, reflecting an acute stress response [27], followed by progressive exploration of the upper zone as habituation occurs. Analysis of the behavioral data revealed that the lowest doses of SP-EMB significantly reduced locomotor activity, as evidenced by decreased total distance traveled and mean swimming speed compared to the 3% DMSO control (*$p < 0.05$; **$p < 0.01$; ****$p < 0.0001$) (Fig. 5). Despite this reduction in locomotion, SP-EMB-treated groups exhibited increased exploratory behavior. Notably, fish exposed to the highest dose showed a significant increase in distance traveled in the upper zone, comparable to DZP (*$p < 0.05$; **$p < 0.01$ vs. control), suggesting an anxiolytic-like effect. Consistently, the time spent in the upper region was significantly increased at doses of 40 and 400 $mg{\cdot}kg^{-1}$, reinforcing the anxiolytic-like profile of the extract.

The anxiolytic activity of SP-EMB may be partially attributed to its phytochemical composition, which is rich in *β*-carboline indole alkaloids, particularly harmane **(8)**, the major constituent. These compounds are known to interact with multiple CNS targets, including benzodiazepine binding sites, thereby modulating anxiety-related behaviors [3,4].

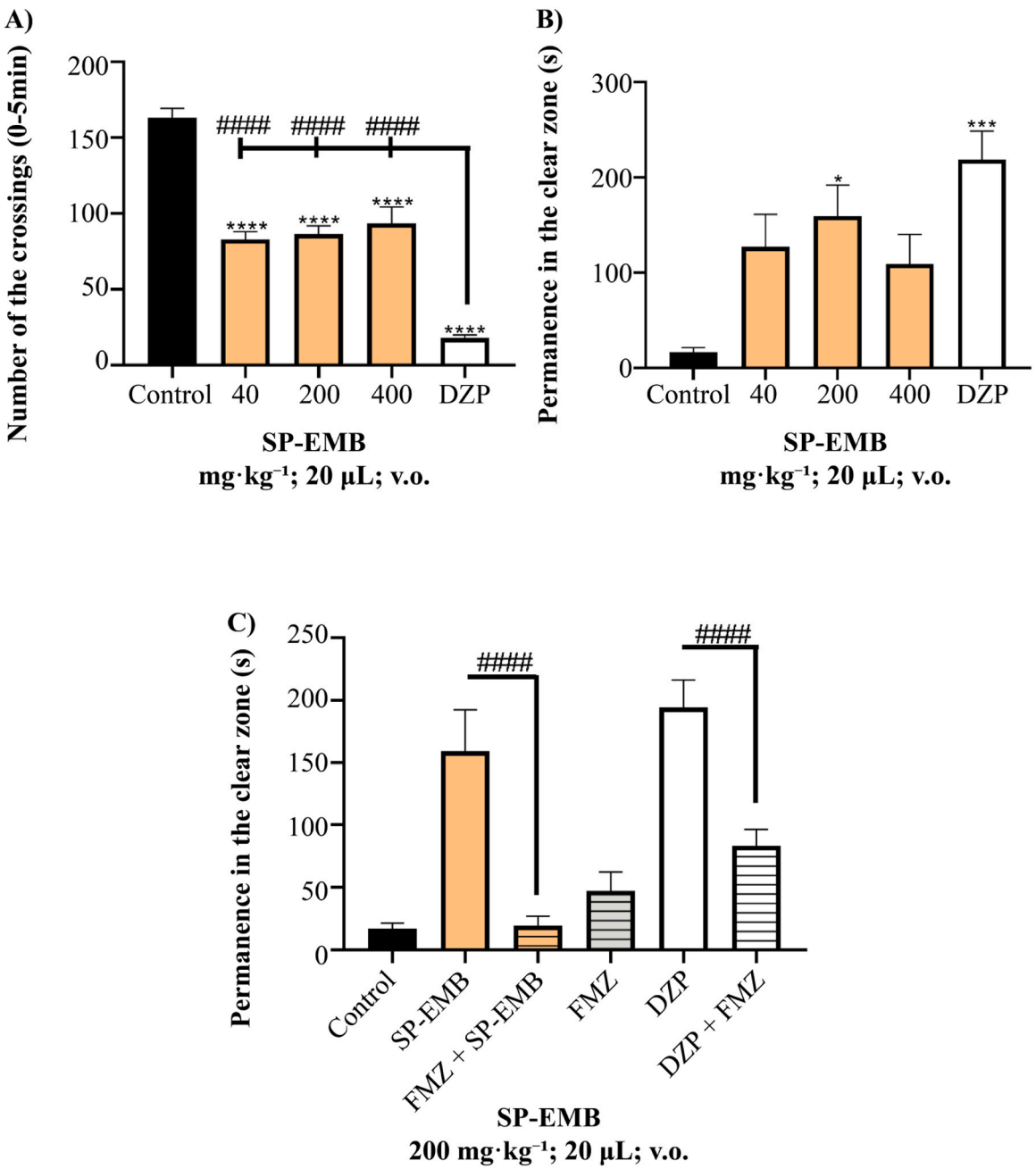

Fig. 3. Effect of SP-EMB on tests of A) locomotion, (**** $p < 0.0001$ vs. Control; #### $p < 0.0001$ vs. DZP), ANOVA followed by *Tukey's* test; B) anxiety, (200 mg·kg^{-1}, *$p < 0.05$, ***$p < 0.001$ vs. Control), Kruskal-Walks followed by *Tukey's* test; and C) GABAergic neuromodulation, (200 mg·kg^{-1}, #### $p < 0.0001$ vs. FMZ+SP-EMB), ANOVA followed by *Tukey's* test.

In agreement with these findings, we previously demonstrated that an alkaloid-rich fraction obtained from *Griffinia* species (Amaryllidaceae) produced marked anxiolytic-like effects in zebrafish in the light/dark test at doses ranging from 40 to 200 mg·kg^{-1} (i.p.). This activity was mainly associated with isoquinoline alkaloids, such as lycorine-, vittatine-, and assoanine-type derivatives, supported by pharmacological antagonism assays and molecular docking analyses indicating interactions with GABA and serotonergic receptors [28].

In addition to alkaloids, the presence of phenylpropanoids may also contribute to the observed anxiolytic effects. Chlorogenic acid **(4)** [29], as well as *p*-coumaric acid [30] and ferulic acid [31] moieties identified within 5-*O*-*p*-coumaroylquinic acid **(6)** and 3-*O*-feruloylquinic acid **(9)**, respectively, have been reported to exert anxiolytic and antioxidant activities. Chlorogenic acid **(4)**, for instance, demonstrated anxiolytic effects in mice using the elevated plus maze, light/dark, and novel object recognition tests in studies involving *Prunus domestica* (Rosaceae) [29]. Likewise, extracts rich in 5-feruloylquinic acid from *Sorbaria tomentosa* (Rosaceae) significantly increased light-area exploration in murine light/dark tests, corroborating its anxiolytic potential [32].

The involvement of the GABAergic system in the anxiolytic effect of SP-EMB was further confirmed using FMZ, a selective benzodiazepine site antagonist at the $GABA_A$ receptor [33]. Pretreatment with FMZ significantly attenuated the anxiolytic-like behavior induced by the lowest effective dose of SP-EMB (200 mg·kg^{-1}; $p < 0.0001$ vs. FMZ + SP-EMB), as evidenced by reduced time spent in the illuminated compartment (Fig. 3C). These results indicate that the anxiolytic action of SP-EMB is mediated, at least in part, through modulation of GABAergic neurotransmission, similarly to classical benzodiazepines

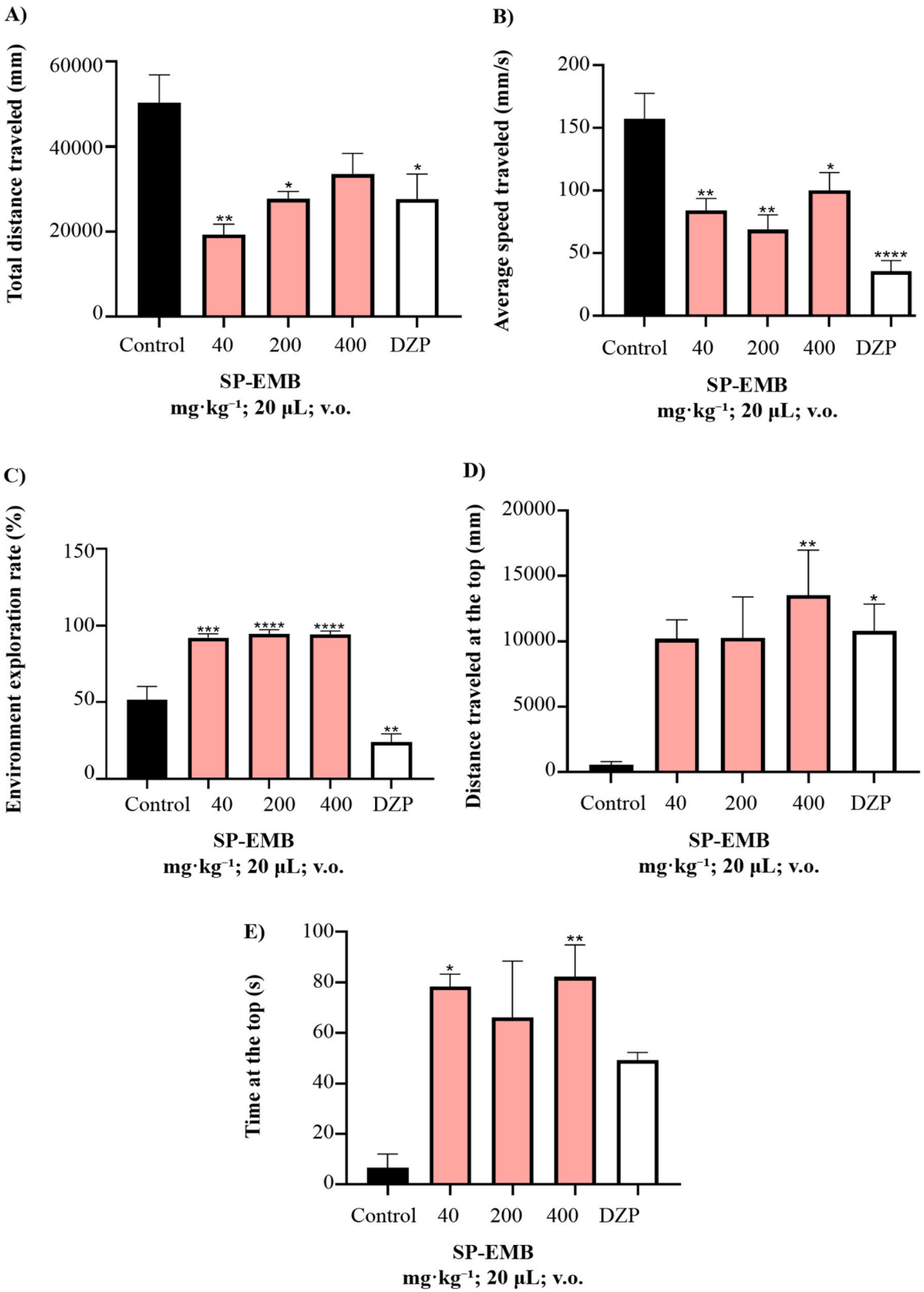

Fig. 5. A) Total distance traveled in the New Tank test under the effect of SP-EMB on zebrafish behavior (0–5 min). B) Total speed traveled in the New Tank test under the effect of SP-EMB on zebrafish behavior (0–5 min). C) Percentage of exploration in the New Tank test under the effect of SP-EMB on zebrafish behavior (0–5 min). D) Distance traveled at the top in the New Tank test under the effect of SP-EMB on zebrafish behavior (0–5 min). E) Time at the top in the New Tank test under the effect of SP-EMB on zebrafish behavior (0–5 min). The values represent the mean ± standard error of the mean for 6 animals/group; using One-way ANOVA followed by *Tukey's* test (A-D) and Kruskal-Wallis followed by *Tukey's* test (E).

commonly used in anxiety treatment [33].

SP-EMB did not attenuate PTZ-induced seizure behavior at any of the evaluated stages (****$p < 0.0001$ vs. Control; ####$p < 0.0001$ vs. DZP), showing a significant difference relative to DZP (4 mg·kg^{-1}), which effectively delayed seizure onset across all three stages when compared with the control groups (Fig. 4).

Seizure generation is primarily associated with disruptions in the excitatory–inhibitory balance within the CNS, particularly involving glutamatergic excitation and γ-aminobutyric acid (GABA)-mediated inhibition [34,35]. While glutamate promotes neuronal excitation, GABA acts to suppress neuronal firing and stabilize neural circuits [36]. In this context, PTZ functions as a potent proconvulsant by enhancing excitatory neurotransmission and reducing GABAergic inhibitory tone [37], thereby inducing rapid-onset seizures that typically require fast-acting anticonvulsant agents. DZP, a positive allosteric modulator of the $GABA_A$ receptor, is widely used in both anxiety and seizure management and thus serves as a suitable positive control in acute seizure models [8].

Although chlorogenic acid **(4)** is abundantly found in plant species with reported neuroprotective and anticonvulsant properties, such as *Morus alba* (Moraceae), its activity in seizure models appears to be context dependent. In electroshock-induced seizure models in mice, which are not exclusively GABAergic, the protective effects of chlorogenic acid have been mainly attributed to its antioxidant and anti-inflammatory properties, whereas the anticonvulsant effects were primarily associated with flavonoids acting on GABAergic pathways [38]. While such neuroprotective mechanisms are relevant for long-term neuronal resilience, they may be insufficient to counteract acute chemically induced seizures, particularly when present at low concentrations, as observed in SP-EMB.

Similarly, phenylpropanoid derivatives structurally related to 5-*O*-*p*-coumaroylquinic acid **(6)** and 3-*O*-feruloylquinic acid **(9)**, have been identified in *Geigeria alata* (Rubiaceae), a species traditionally employed

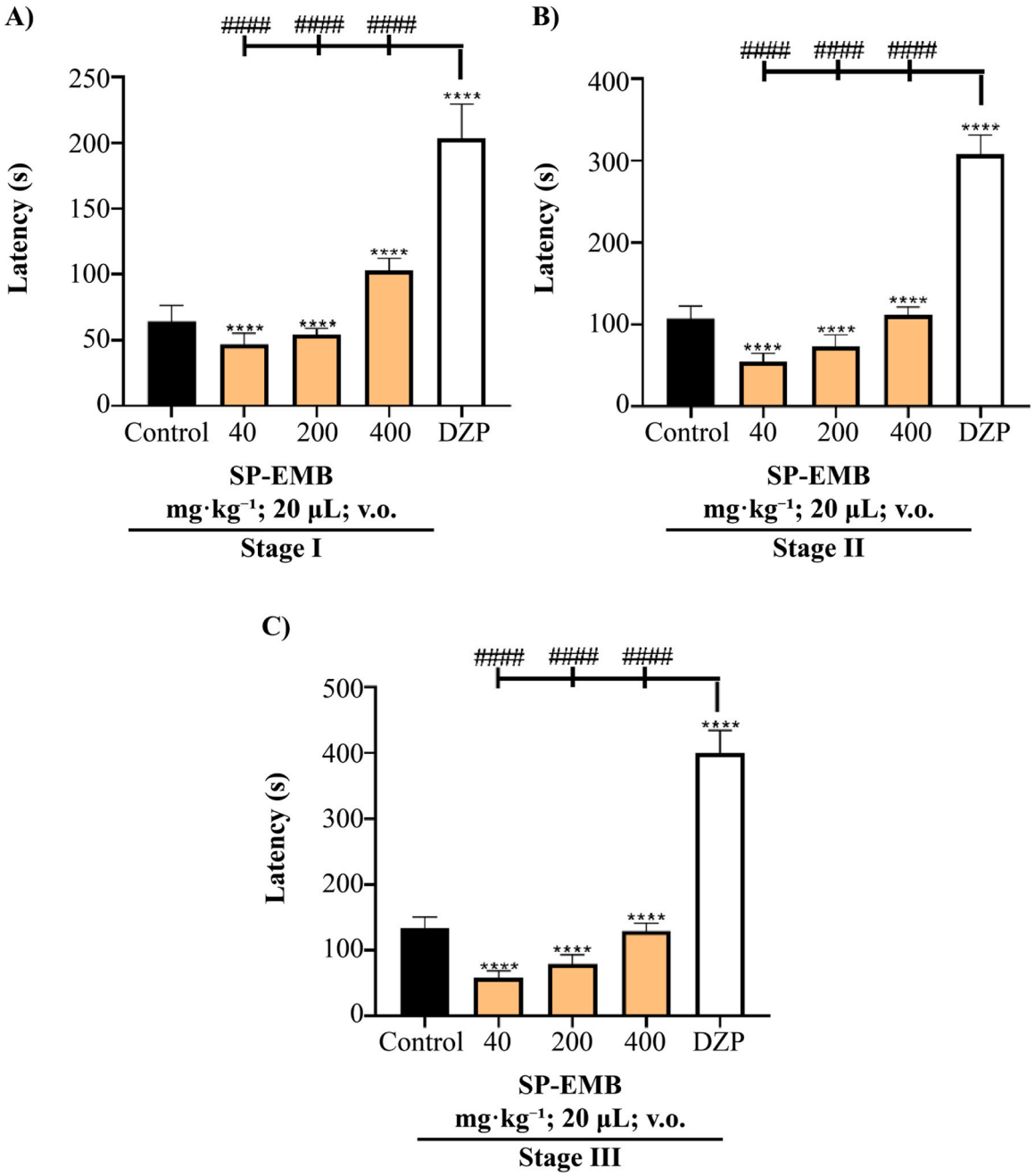

Fig. 4. Effect of SP-EMB on seizure tests in stages A) I, B) II and C) III. (**** $p < 0.0001$ vs Control; #### $p < 0.0001$ vs DZP). ANOVA followed by *Tukey's* test.

in epilepsy treatment; however, the specific bioactive constituents responsible for this ethnopharmacological use have not yet been elucidated [39]. In contrast, studies on *Aster glehni* (*Asteraceae*) have demonstrated that caffeoyl and *p*-coumaroyl (3-*O*-*p*-coumaroylquinic) moieties, contributed to the attenuation of PTZ-induced seizures in mice, an effect primarily attributed to antioxidant-mediated neuroprotection rather than direct modulation of inhibitory neurotransmission [37,40].

Regarding alkaloid constituents, the β-carboline harmane **(8)** has been reported to act either as an agonist or antagonist at the benzodiazepine binding site within the $GABA_A$ receptor complex [41,42]. Harmane **(8)** has shown significant, dose-dependent anticonvulsant effects in maximal electroshock seizure models; however, in PTZ-induced seizure paradigms, higher doses exacerbated seizure severity. This dual behavior suggests that harmane **(8)** may exert protective effects in generalized tonic–clonic seizure models while displaying a narrow therapeutic window or even proconvulsant activity in absence-type (petit mal) seizures [43]. In the present study, no anticonvulsant effect was observed in zebrafish, a model increasingly used in epilepsy research due to its high genetic homology with humans, including approximately 70% overall genomic similarity and the expression of 84% of genes associated with human diseases in *Danio rerio* [44–46].

Taken together, the lack of anticonvulsant activity observed for SP-EMB may be attributed to the inability of its major constituent, harmane **(8)**, to sufficiently counterbalance the complex excitatory neurotransmitter release triggered by PTZ, despite its modulatory interaction with the $GABA_A$ receptor. Additionally, chlorogenic acid **(4)**, 5-*O*-*p*-coumaroylquinic acid **(6)** and 3-*O*-feruloylquinic acid **(9)** exhibit pharmacological profiles more closely related to neuroprotection and inflammation modulation than to acute seizure suppression.

3.3. Docking-Guided Identification of Putative GABAergic Ligands

To elucidate which constituents might underlie the anxiolytic activity mediated by the GABAergic system, molecular docking simulations were conducted using the target protein of interest. At the conclusion of the simulations, all ligands, including DZP, presented root mean square deviation (RMSD) values below 2.0 Å (Tab. S2), indicating satisfactory pose stability and reproducibility of the docking protocol [47]. Accordingly, the lowest-energy binding poses, corresponding to the most favorable ligand–protein interactions, were selected for further analysis.

Integration of RMSD (Å) and binding affinity energy (kcal·mol^{-1}) values allowed the identification of two major clusters. Cluster I comprised compounds exhibiting both low positional deviation (RMSD < 1.6 Å) and high binding affinity ($\Delta G < -7.8$ kcal·mol^{-1}). Within this group, harmane **(8)** showed an RMSD of 1.34 Å and a binding free energy of -8.279 kcal·mol^{-1} (Fig. 6), indicating a stable interaction with the $GABA_A$ receptor. Notably, harmane **(8)** occupied the same benzodiazepine binding pocket as DZP, located in the extracellular domain of the receptor (Fig. 7A).

Cluster II displayed a higher density of data points, particularly for canthosides C and D **(1)** (blue spectrum), with RMSD values around 1.4 Å and binding affinity energies near -7.1 kcal·mol^{-1}, suggesting consistent convergence toward similar binding conformations and reinforcing the robustness of the docking results within this group.

In addition, chlorogenic acid compound **(4)** exhibited docking parameters comparable to those of the DZP agonist, including RMSD values between 1.5 and 1.6 Å and binding affinity energies of -7.05 and -6.658 kcal·mol^{-1}, respectively (Fig. 6). Importantly, this compound also occupied the benzodiazepine binding site (Fig. 7A), indicating potential competitive interaction with DZP at the $GABA_A$ receptor.

At the end of the independent molecular docking simulation cycle, the extract's ligands are distributed across multiple $GABA_A$ receptor binding sites, suggesting a possible allosteric effect through synergism. Pocket I (DZP site) shows competitive binding among the ligands 5-*O*-*p*-coumaroylquinic acid, chlorogenic acid, and harmane (Fig. 7A). In a neighboring site (Pocket II), the compounds strictosidine, canthoside C-D, strictosidinic acid, and ophiorine A bind (Fig. 7B), interacting with residues near the DZP binding site. In the less frequent sites (Fig. 7C, D), the compounds lyalosidic acid and hydroxy-methoxy-benzoic acid-*O*-pentosyl hexoside (Pocket III) and 3-*O*-feruloylquinic acid and ophiorine B (Pocket IV) bind. Specifically, the compounds in Pocket IV bind to the transmembrane domain, interacting with residues within the receptor channel (Fig. 7D). In contrast, the other compounds are distributed in the extracellular binding domains, with pockets I and II associated with allosteric modulation of the $GABA_A$ receptor, located between the α1-D and γ2-C subunits and characterized as DZP agonist binding sites [48].

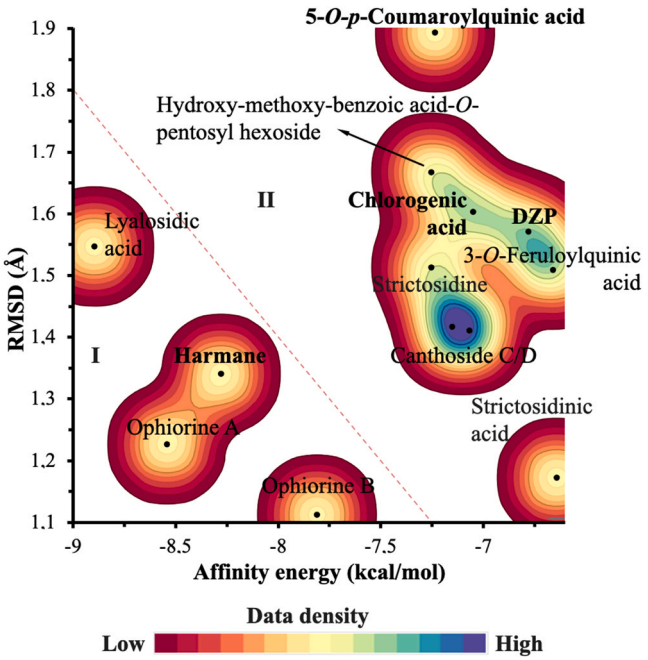

Fig. 6. Distribution of compounds in a space defined by binding affinity energy (kcal·mol^{-1}) and RMSD (Å). Clusters I and II indicate distinct energy states, associated with different binding modes. Compounds such as harmane **(8)**, ophiorine A **(3)**, ophiorine B **(5)** and lyalosidic acid **(10)** are concentrated in regions of lower RMSD, suggesting greater structural stability, while chlorogenic acid **(4)** and DZP occupy regions with greater conformational dispersion. The arrow indicates the transition associated with the canthoside C or D **(1)** site, highlighting changes in the energy and conformational profile of the ligands analyzed.

Analysis of the binding modes revealed the presence of three distinct binding pockets. Pocket I corresponds to the classical benzodiazepine (DZP) binding site, located in the extracellular domain at the interface between the α1-D and γ2-C subunits of the $GABA_A$ receptor (Fig. 8B) [12]. Within this pocket, chlorogenic acid **(4)**, 5-*O*-*p*-coumaroylquinic acid **(6)**, and harmane **(8)** were accommodated, indicating that these compounds may adopt a benzodiazepine-like binding mode at the $GABA_A$ receptor (Fig. 8C). In contrast, Pocket II was preferentially occupied by the structurally more complex analogues canthoside C or D **(1)**, strictosidinic acid **(12)**, and strictosidine **(13)** (Fig. 8B), suggesting that this region may favor ligands with increased three-dimensional complexity.

Detailed analysis of ligand–protein interactions revealed that harmane **(8)**, an amine-containing heteroaromatic compound, established several interactions in common with DZP (Fig. 8D). Its aromatic scaffold enabled π–π stacking interactions with the phenyl ring of Phe77, as well as hydrophobic (van der Waals) interactions with the aromatic side chains of Tyr58 and Tyr160. These residues have been reported as key determinants in the recognition of novel $GABA_A$ modulators that target the benzodiazepine binding site (Fig. 8D) [12,49].

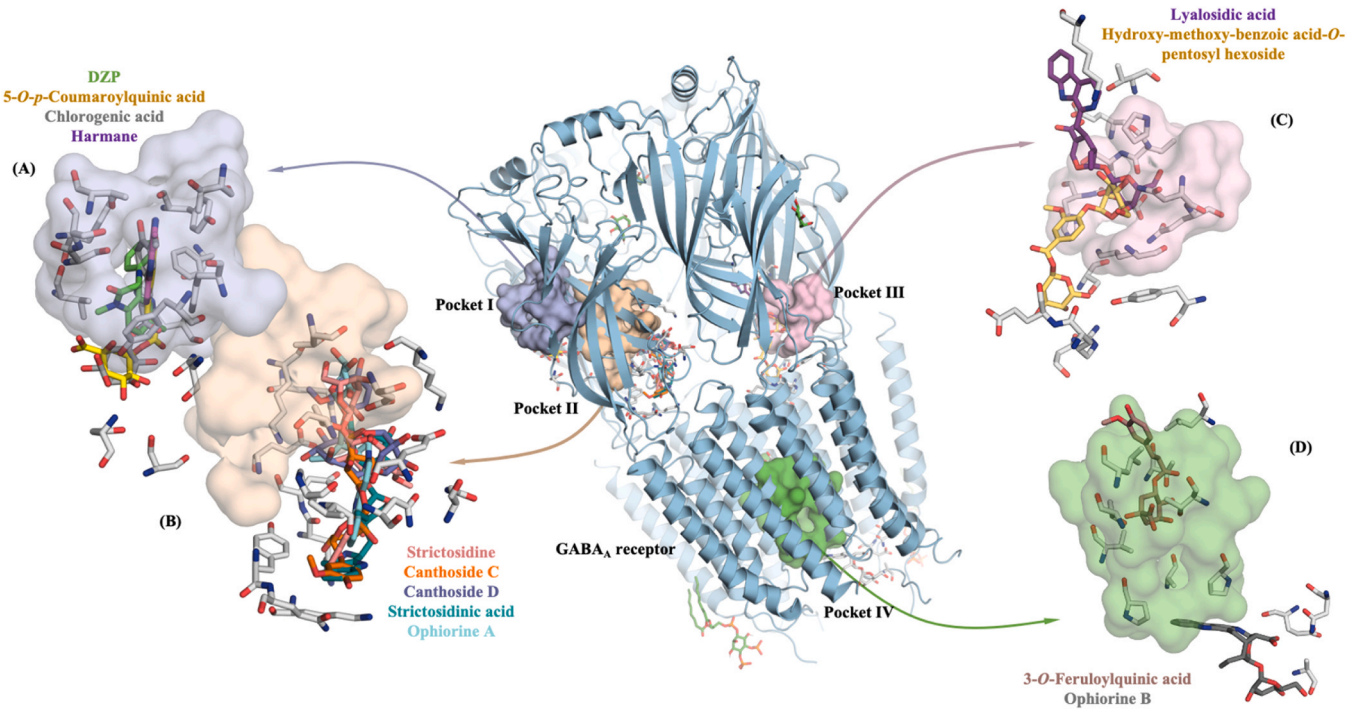

Fig. 7. Occupation of phytochemicals from the extracts distributed among the binding pockets, after the end of the molecular docking simulations: A) in pocket I, the ligands 5-*O*-*p*-coumaroylquinic acid, chlorogenic acid, and harmane complexed at the same binding site as the agonist DZP; B) in pocket II, the ligands strictosidine, canthoside C/D, strictosidinic acid, and ophiorine A complexed; C) in pocket III, the ligands lyalosidic acid and hydroxy-methoxy-benzoic acid-*O*-pentosyl hexoside complexed; and D) in pocket IV, the ligands 3-*O*-feruloylquinic acid and ophiorine B complexed.

Similarly, the cinnamic acid-derived phenylpropanoids chlorogenic acid **(4)** and 5-*O*-*p*-coumaroylquinic acid **(6)** also possess aromatic centers that preferentially interact with Phe77 (Fig. 8E). However, when compared with DZP and harmane **(8)**, these compounds displayed a more flexible binding mode, likely due to their larger size and higher conformational freedom.

In addition, harmane **(8)** formed a hydrogen bond with the polar side chain of Thr207, with a strong contribution from its secondary amine (Nsp^2–H). In contrast, the glycosidic moieties of chlorogenic acid **(4)** and 5-*O*-*p*-coumaroylquinic acid **(6)** engaged in hydrogen bonding interactions with Tyr58 and Asn60. The observed donor–acceptor distances (> 2.25 Å) suggest moderately strong yet reversible interactions, a feature commonly associated with transient ligand–receptor complexes and favorable pharmacological modulation (Tab. S2) [50].

Taken together, molecular docking simulations identified harmane **(8)** and chlorogenic acid **(4)** as the main contributors to the observed anxiolytic activity, based on their favorable binding profiles at the $GABA_A$ receptor. Both compounds establish stabilizing hydrophobic interactions with the Phe77 residue, a key amino acid widely implicated in the recognition and modulation of benzodiazepine-sensitive $GABA_A$ receptor ligands.

3.4. Assessment of anxiolytic-like of chlorogenic acid (4) and harmane (8)

Based on the molecular docking results, which identified chlorogenic acid **(4)** and harmane **(8)** as the ligands with the most favorable binding profiles at the $GABA_A$ receptor, both compounds were selected for *in vivo* evaluation of their anxiolytic-like effects and toxicity in adult zebrafish. In this regard, chlorogenic acid **(4)** and harmane **(8)**, administered at 4, 20, and 40 $mg{\cdot}kg^{-1}$, did not induce acute toxicity after 96 h of exposure (Tab. S3). Indeed, no significant mortality, behavioral alterations, or anatomical abnormalities were observed compared with the control group ($p > 0.05$), indicating an estimated LD_{50} greater than 40 $mg{\cdot}kg^{-1}$ and a favorable acute safety profile under the experimental conditions. These findings corroborate previous reports describing the low toxicity of chlorogenic acid and harmane within pharmacologically relevant concentration ranges [51,52].

In the locomotor activity test, chlorogenic acid and harmane (Figs. 9A and 9B) did not produce significant alterations in zebrafish swimming behavior compared with the control group, indicating the absence of sedative or stimulant effects on the locomotor system. No relevant changes in locomotion patterns were observed relative to either the positive or negative controls. These findings are particularly relevant when interpreted alongside the light/dark test results, as they indicate that the increased time spent in the illuminated compartment was not associated with locomotor impairment or immobility, but rather with a specific modulation of anxiety-like behavior. Thus, the data support an anxiolytic-like effect without significant interference in zebrafish locomotion.

In the light and dark test, harmane promoted an increase in the time spent in the light zone at doses of 20 and 40 $mg{\cdot}kg^{-1}$ compared to the control, with progressive statistical significance, being more pronounced at the dose of 40 $mg{\cdot}kg^{-1}$. This effect was comparable to that observed in the group treated with DZP (4 $mg{\cdot}kg^{-1}$), which showed the longest time spent in the light region, characterizing a typical profile of anxiolytic effect (Fig. 9D). Similarly, chlorogenic acid also induced a significant increase in time spent in the light zone, but only at the dose of 40 $mg{\cdot}kg^{-1}$, approaching the response observed for DZP (Fig. 9C). Statistical differences were also observed in relation to DZP at doses of 4 and 20 $mg{\cdot}kg^{-1}$, suggesting a distinction between treated groups and the positive control, indicating that these doses did not reproduce a similar effect to DZP. Therefore, the results indicate that both harmane and chlorogenic acid exhibit dose-dependent anxiolytic activity, although with lower efficacy than the positive control, especially at lower doses.

Regarding the neuromodulation test, the results indicate that only chlorogenic acid, at a dose of 40 $mg{\cdot}kg^{-1}$, exerts an anxiolytic effect in adult zebrafish through modulation of the GABAergic system, specifically via interaction with GABA type A ($GABA_A$) receptors. This

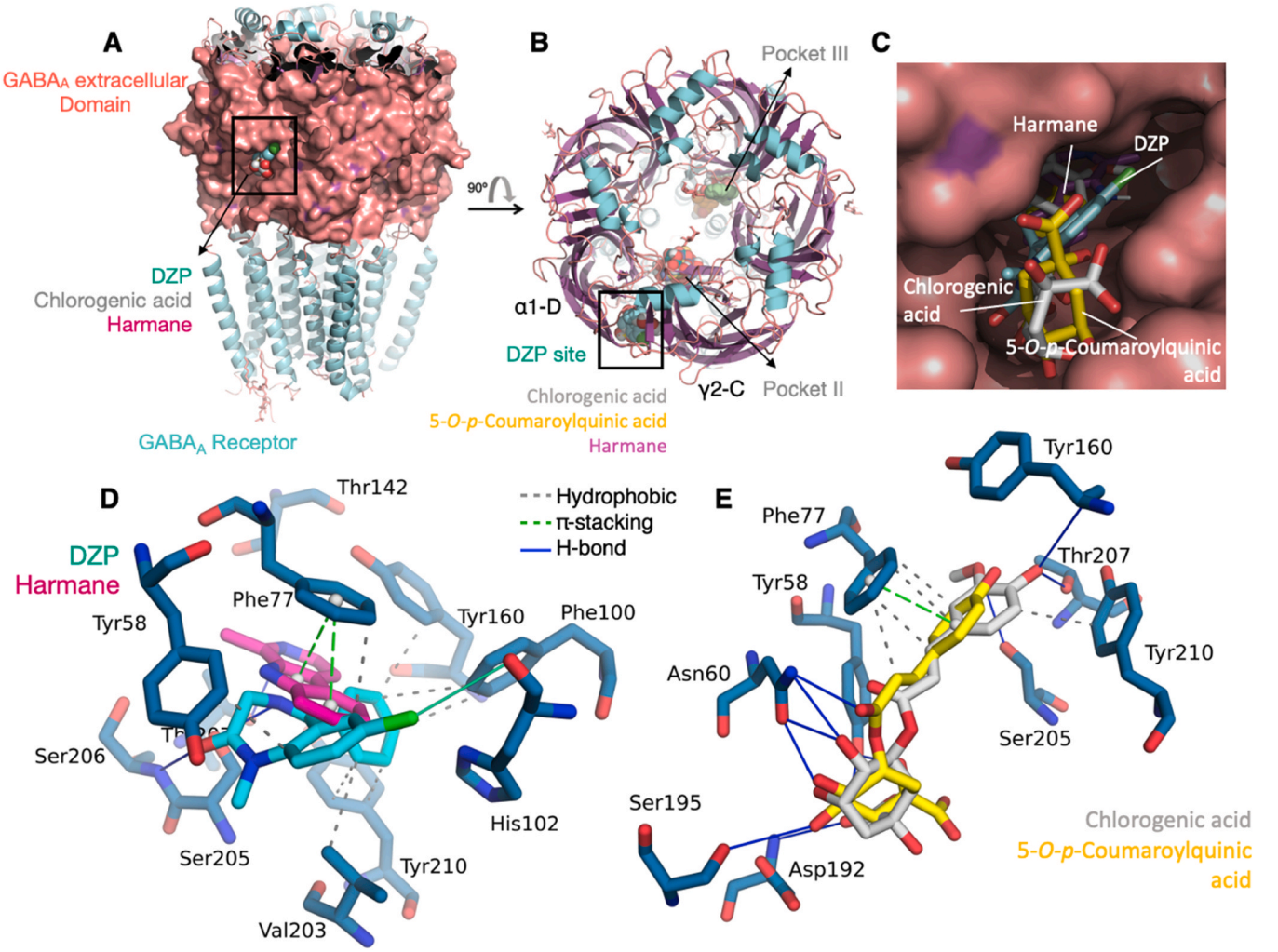

Fig. 8. A) Three-dimensional visualization of the coupling of the leading compounds to the DZP binding domain in the GABA$_A$ receptor, with B) visualization of the top of the occupation of the other ligands through the GABA$_A$ receptor binding sites. C) Three-dimensional visualization of the binding mode of the ligands DZP (GABA$_A$ agonist), harmane **(8)**, chlorogenic acid **(4)** and 5-*O*-*p*-coumaroylquinic acid **(6)**. Ligand-protein interactions formed between the residues of the GABA$_A$ receptor binding site (blue color) and the ligands D) DZP, harmane **(8)**, E) chlorogenic acid **(4)** and 5-*O*-*p*-coumaroylquinic acid **(6)**.

inference is supported by the pretreatment experiment with FMZ (4 mg·kg^{-1}), a competitive antagonist of benzodiazepine sites on GABA$_A$ receptors.

In Fig. 9E, related to the GABAergic mechanism of chlorogenic acid, it can be seen that pretreatment with FMZ significantly reversed the increase in time spent in the light zone induced by the samples. While the groups treated only with the samples (40 mg·kg^{-1}) showed anxiolytic behavior (longer time in the light zone), the groups that received FMZ before the samples remained in the dark zone for most of the time, a typical anxiety behavior in zebrafish. This reversal effect indicates that the anxiolytic action of chlorogenic acid is dependent on the activation of GABA$_A$ receptors, being blocked by the antagonist FMZ (chlorogenic acid + FMZ vs chlorogenic acid #p < 0.05). This mechanism is also observed for DZP (positive control), a classic benzodiazepine that potentiates the action of GABA at GABA$_A$ receptors (DZP + FMZ vs DZP ##p < 0.01). Bouayed *et al.* (2007) demonstrated that chlorogenic acid isolated from fruits showed an anxiolytic effect in mice, partially mediated by interaction with GABA$_A$ receptors. Unlike chlorogenic acid, harmane did not show an anxiolytic effect mediated by the GABAergic system in the assays (Fig. 9F). This suggests that the anxiolytic mechanism of action of harmane may involve other neurochemical pathways not directly associated with GABA$_A$ receptors, such as the serotonergic pathway (5-HT). [53]

4. Conclusion

UPLC-ESI-QToF-MS/MS profiling of the methanolic bark extract of *Simira paraensis* (SP-EMB) enabled the annotation of *β*-carboline alkaloids, phenolic acids, and phenolic glycosides, with harmane **(8)** identified as the major constituent. Behavioral assays in adult zebrafish demonstrated that SP-EMB exhibits a consistent anxiolytic-like profile without acute toxicity at the tested doses (LD_{50} > 400 mg·kg^{-1}). In the light/dark test, the intermediate dose of SP-EMB (200 mg·kg^{-1}) produced the most pronounced anxiolytic-like effect, whereas in the novel tank test the extract increased exploratory behavior in the upper zone, particularly at 40 and 400 mg·kg^{-1}, supporting its anxiolytic-like activity across complementary behavioral models.

Mechanistically, the anxiolytic effect of SP-EMB was partially associated with modulation of the GABAergic system, as evidenced by the reversal of the behavioral effects after FMZ pretreatment. Molecular docking analyses further supported these findings by demonstrating favorable interactions of harmane **(8)** and chlorogenic acid **(4)** with the benzodiazepine-binding site of the GABA$_A$ receptor. Based on these *in silico* results, both compounds were subsequently evaluated *in vivo* and displayed low acute toxicity (LD_{50} > 40 mg·kg^{-1}) and dose-dependent anxiolytic-like effects without significant impairment of locomotor activity. Harmane induced significant anxiolytic-like effects at 20 and

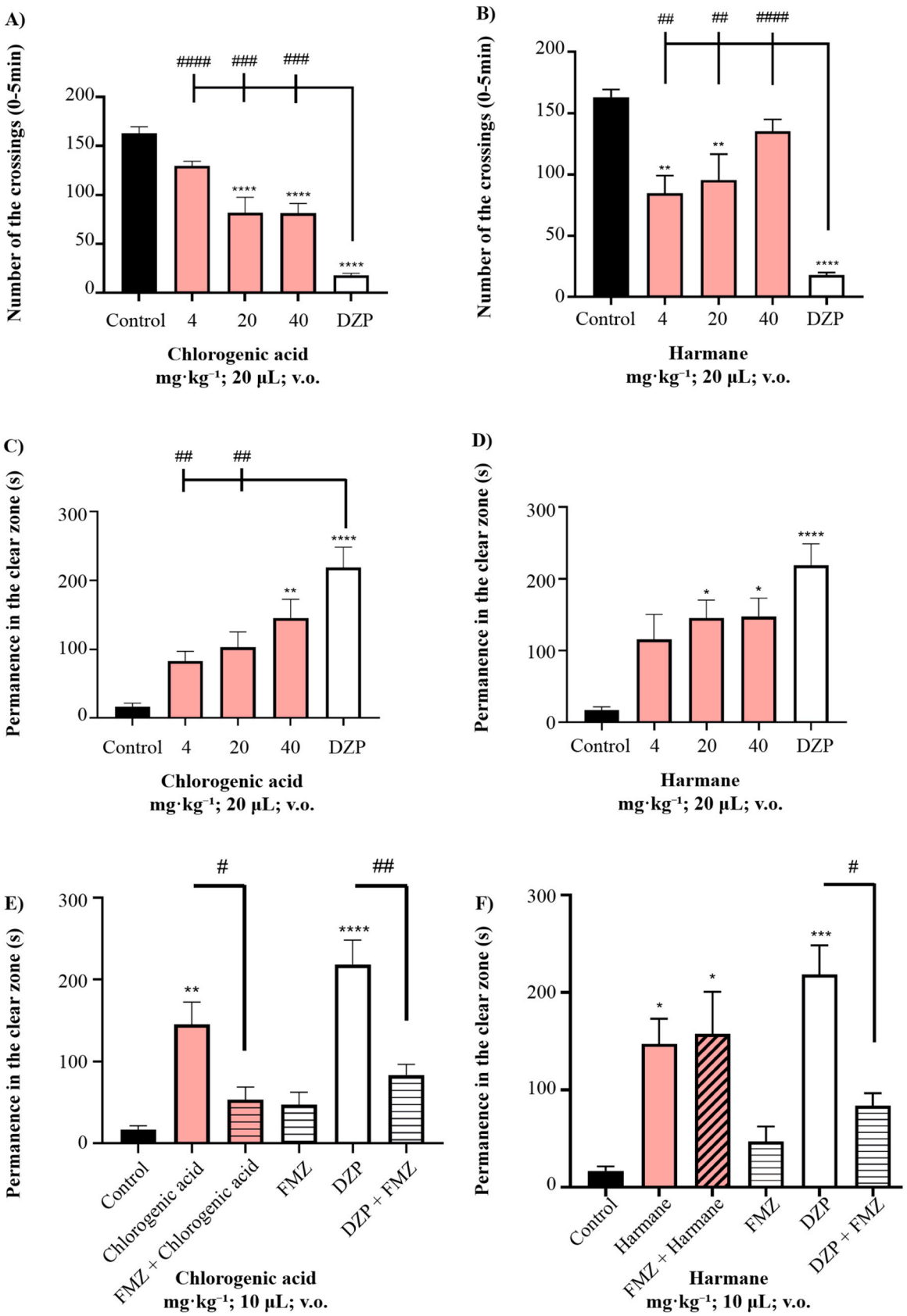

Fig. 9. Effect of harmane (A) and chlorogenic acid (B) samples on the locomotor behavior of adult zebrafish in the Open Field Test (0–5 min), (****$p < 0.0001$ vs. Control). Effect of harmane (C) and chlorogenic acid (D) samples on zebrafish anxiety in the light/dark test (0–5 min), (*$p < 0.5$, **$p < 0.1$, ****$p < 0.0001$ vs. Control; ##$p < 0.01$ vs. DZP). Effect of harmane (A) and chlorogenic acid (B) samples on GABAergic neuromodulation in zebrafish in the light/dark test (0–5 min). Values represent the mean ± standard error of the mean for 6 animals/group; ANOVA followed by *Tukey's* test (A-D) and two-way ANOVA followed by *Tukey's* test (E and F) were adopted.

40 mg·kg^{-1}, whereas chlorogenic acid was effective mainly at 40 mg·kg^{-1}. In addition, chlorogenic acid showed anxiolytic activity mediated by $GABA_A$ receptors, whereas harmane appeared to involve additional neurochemical pathways, possibly related to serotonergic modulation.

Overall, our study provides experimental and mechanistic evidence supporting the potential of *Simira paraensis* extract and its constituents as promising sources of anxiolytic agents with reduced sedative effects compared with commercial drugs.

CRediT authorship contribution statement

Larissa Rodrigues Jales Martins: Formal analysis, Methodology, Investigation, Writing – original draft, Writing – review & editing. **Nadia Eligia Nunes Pinto Paracampo:** Conceptualization, Funding acquisition, Resources, Writing – original draft. Paulo Riceli Vasconcelos Ribeiro: Data curation, Methodology, Formal analysis, Investigation. **Francisco Oiram Filho:** Methodology, Formal analysis. **Amanda Maria Barros Alves:** Formal analysis, Investigation. **Hélcio Silva dos Santos:** Investigation, Methodology, Funding acquisition, Writing – original draft. **Jane Eire Silva Alencar de Menezes:** Investigation, Supervision, Funding acquisition, Writing – original draft. **Márcia Machado Marinho:** Supervision, Validation, Writing – original draft. **Matheus Nunes da Rocha:** Formal analysis. **Emmanuel Silva Marinho:** Methodology, Supervision, Funding acquisition, Writing – original draft. **Kirley Marques Canuto:** Conceptualization, Supervision, Project administration, Funding acquisition, Writing – original draft, Writing – review & editing.

Ethical approval for the use of animals

The analyses on zebrafish were performed in accordance with international principles for the use and care of laboratory animals, as well as Brazilian Law 11.794, of October 8, 2008, Decree 6.899, of July 15, 2009, and the regulations of the National Council for the Control of Animal Experimentation (CONCEA), under protocol CEUA 4.055.051.018 (ID 000.639) and, finally, approved by the Ethics Committee on the Use of Animals of the State University of Ceará (CEUA-UECE; nº 04983945/2021).

Declaration of Competing Interest

The authors declare that they have no known competing financial interests or personal relationships that could have appeared to influence the work reported in this paper.

Acknowledgments

The authors thank Embrapa (SEG 10.22.02.002.00.02.00), FAPESPA and CNPQ-UNIVERSAL [#407457/2025–9] for financial support, FUNCAP (BMD-0008-02718.01.07/24) and CAPES for granting a master's scholarship to L.R.J. Martins, and CNPq for the research grants awarded to K.M. Canuto [# 312252/2025–0] and E.S. Marinho [# 309349/2025–7].

Appendix A. Supporting information

Supplementary data associated with this article can be found in the online version at doi:10.1016/j.jpba.2026.117602.

References

[1] D. Martins, C.V. Nunez, Secondary metabolites from rubiaceae species, Molecules 20 (2015) 13422–13495, https://doi.org/10.3390/molecules200713422.
[2] V.F. Moreira, I.J.C. Vieira, R. Braz-Filho, Chemical constituents and biological activities of simira genus: a contribution to the chemotaxonomic of rubiaceae family, Nat. Prod. J. 4 (2014) 290–298.
[3] R. Cao, W. Peng, Z. Wang, A. Xu, β-carboline alkaloids: biochemical and pharmacological functions, Curr. Med. Chem. 14 (2007) 479–500, https://doi.org/10.2174/092986707779940998.
[4] L. Yu, N. Shen, J. Ren, H. Xin, Y. Cui, Resource distribution, pharmacological activity, toxicology and clinical drugs of β-Carboline alkaloids: an updated and systematic review, Fitoterapia 180 (2025) 106326, https://doi.org/10.1016/j.fitote.2024.106326.
[5] E. Tadros, S. Keerthana, S. Padder, J. Totlani, D. Hirsch, D.N. Kaidbay, L. Contreras, A. Naqvi, S. Miles, K. Mercado, A. Meyer, S. Renteria, R.N. Pechnick, I. Danovitch, W.W. IsHak, Anxiety disorders, PTSD and OCD: systematic review of approved psychiatric medications (2008–2024) and pipeline phase III medications, 2024-11–2, Drugs Context. 14 (2025), https://doi.org/10.7573/dic.2024-11-2.
[6] J. Sarris, Herbal medicines in the treatment of psychiatric disorders: 10-year updated review, Phytother. Res. 32 (2018) 1147–1162, https://doi.org/10.1002/ptr.6055.
[7] M.R.D.V. Barbosa, A.L. Peixoto, As espécies de Simira (Rubiaceae, Rondeletieae) da Amazônia Brasileira, Acta Amaz. 19 (1989) 27–46, https://doi.org/10.1590/1809-43921989191046.
[8] M.K.A. Ferreira, A.W. Da Silva, A.L. Dos Santos Moura, K.V.B. Sales, E.M. Marinho, J. Do Nascimento Martins Cardoso, M.M. Marinho, P.N. Bandeira, F.E. A. Magalhães, E.S. Marinho, J.E.S.A. De Menezes, H.S. Dos Santos, Chalcones reverse the anxiety and convulsive behavior of adult zebrafish, Epilepsy Behav. 117 (2021) 107881, https://doi.org/10.1016/j.yebeh.2021.107881.
[9] A.L.P. Moreira, A.C. Luchiari, Effects of oxybenzone on zebrafish behavior and cognition, Sci. Total. Environ. 808 (2022) 152101, https://doi.org/10.1016/j.scitotenv.2021.152101.
[10] J.M. Guedes, M.K.A. Ferreira, L.S. Oliveira, A.W. da Silva, J.E.S.A. de Menezes, P. N. Bandeira, A.M.R. Teixeira, E.M. Marinho, M.M. Marinho, E.S. Marinho, H.S. dos Santos, Anxiolytic-like Effect in Adult Zebrafish (Danio rerio) through GABAergic System and Molecular Docking Study of Chalcone (E)-1-(2-hydroxy-3,4,6-trimethoxyphenyl)-3-(4-methoxyphenyl)prop-2-en-1-one, Biointerface Res. Appl. Chem. 13 (2022) 15, https://doi.org/10.33263/BRIAC131.015.
[11] T.A. Halgren, Merck molecular force field. I. Basis, form, scope, parameterization, and performance of MMFF94, J. Comput. Chem. 17 (1996) 490–519, https://doi.org/10.1002/(SICI)1096-987X(199604)17:5/6%3C490::AID-JCC1%3E3.0.CO;2-P.
[12] S. Masiulis, R. Desai, T. Uchański, I. Serna Martin, A. Et, GABAA receptor signalling mechanisms revealed by structural pharmacology, Nature (2019), https://doi.org/10.1038/s41586-018-0832-5.
[13] G.M. Morris, R. Huey, W. Lindstrom, M.F. Sanner, R.K. Belew, D.S. Goodsell, A. J. Olson, AutoDock4 and AutoDockTools4: Automated docking with selective receptor flexibility, J. Comput. Chem. 30 (2009) 2785–2791, https://doi.org/10.1002/jcc.21256.
[14] E.M. Marinho, J. Batista de Andrade Neto, J. Silva, C. Rocha da Silva, B. C. Cavalcanti, E.S. Marinho, H.V. Nobre Júnior, Virtual screening based on molecular docking of possible inhibitors of Covid-19 main protease, Microb. Pathog. 148 (2020) 104365, https://doi.org/10.1016/j.micpath.2020.104365.
[15] T. Kanchanapoom, R. Kasai, K. Yamasaki, Iridoid and phenolic diglycosides from *Canthium berberidifolium*, Phytochemistry 61 (2002) 461–464, https://doi.org/10.1016/S0031-9422(02)00140-1.
[16] S. Squara, A. Caratti, A. Fina, E. Liberto, N. Koljančić, I. Špánik, G. Genova, G. Castello, C. Bicchi, A. De Villiers, C. Cordero, Artificial intelligence decision making tools in food metabolomics: Data fusion unravels synergies within the hazelnut (Corylus avellana L.) metabolome and improves quality prediction, Food Res. Int. 194 (2024) 114873, https://doi.org/10.1016/j.foodres.2024.114873.
[17] C. Bitwell, S.I. Sen, C. Luke, M.K. Kakoma, UHPLC-MS/MS phytochemical screening, polyphenolic content and antioxidant potential of Diplorhynchus condylocarpon (Müll.Arg.) Pichon (Apocynaceae), a medicinal plant, Sci. Afr. 20 (2023) e01712, https://doi.org/10.1016/j.sciaf.2023.e01712.
[18] M.N. Clifford, K.L. Johnston, S. Knight, N. Kuhnert, Hierarchical Scheme for LC-MSn Identification of Chlorogenic Acids, J. Agric. Food Chem. 51 (2003) 2900–2911, https://doi.org/10.1021/jf026187q.
[19] M.N.G. Sanches, Estudo fitoquímico e biológico de Simira grazielae (Rubiaceae), Phytochemical and biological study of Simira grazielae (Rubiaceae) (2019). ⟨https://rima.ufrrj.br/jspui/handle/20.500.14407/10243⟩ (accessed June 9, 2025).
[20] R. Aquino, L. Garofalo, N.D. Tommasi, O.L.D. Ugaz, C. Pizza, Glucoindole alkaloids from bark of two Sickingia species, Phytochemistry 37 (1994) 1471–1475, https://doi.org/10.1016/S0031-9422(00)90436-9.
[21] A.B.F.D'O. Bastos, M.G.D. Carvalho, J.R. Velandia, R. Braz-Filho, Constituintes químicos isolados de simira glaziovii (K. schum) steyerm. e a atribuição dos deslocamentos químicos dos átomos de carbono e hidrogênio do alcalóide ofiorina e seus derivados, QuíM. Nova 25 (2002) 241–245, https://doi.org/10.1590/S0100-40422002000200012.
[22] S. Li, W. Liu, L. Teng, X. Cheng, Z. Wang, C. Wang, Metabolites identification of harmane in vitro/in vivo in rats by ultra-performance liquid chromatography combined with electrospray ionization quadrupole time-of-flight tandem mass spectrometry, J. Pharm. Biomed. Anal. 92 (2014) 53–62, https://doi.org/10.1016/j.jpba.2014.01.003.
[23] H. Seki, A. Hashimoto, T. Hino, The ^{1}H- and ^{13}C-Nuclear Magnetic Resonance Spectra of Harman. Reinvestigation of the Assignments by One- and Two-Dimensional Methods, (1993). ⟨https://www.jstage.jst.go.jp/article/cpb1958/41/6/41_6_1169/_article/-char/ja/⟩ (accessed May 7, 2026).
[24] M. Duran-Izquierdo, L. Sierra-Marquez, M. Taboada-Alquerque, J. Olivero-Verbel, Simira cordifolia protects against metal induced-toxicity in Caenorhabditis elegans, Front. Pharmacol. 14 (2023) 1235190, https://doi.org/10.3389/fphar.2023.1235190.

[25] Drug Development and Therapeutics - View PDF, Drug Dev. Ther. (n.d.). ⟨https://ddtjournal.net/view-pdf/⟩ (accessed January 24, 2026).
[26] N.G.G. Gonçalves, J.I.F. De Araújo, F.E.A. Magalhães, F.R.S. Mendes, M.D.P. Lobo, A.C.D.O.M. Moreira, R.D.A. Moreira, Protein fraction from Artocarpus altilis pulp exhibits antioxidant properties and reverses anxiety behavior in adult zebrafish via the serotoninergic system, J. Funct. Foods 66 (2020) 103772, https://doi.org/10.1016/j.jff.2019.103772.
[27] S. Tran, A. Facciol, R. Gerlai, Alcohol-induced behavioral changes in zebrafish: The role of dopamine D2-like receptors, Psychopharmacol. (Berl.) 233 (2016) 2119–2128, https://doi.org/10.1007/s00213-016-4264-3.
[28] E.L.L. Leite, A. Sheila De Queiroz Souza, P. Riceli Vasconcelos Ribeiro, R. De Cássia Alves Pereira, N. Florêncio Martins, M. Kueirislene Amâncio Ferreira, J.E. Silva Alencar De Menezes, H. Silva Dos Santos, O. Deusdênia Loiola Pessoa, K. Marques Canuto, Molecular Docking and GC/MS-Based Approach for Identification of Anxiolytic Alkaloids from *Griffinia* (Amaryllidaceae) Species in a Zebrafish Model, Chem. Biodivers. 21 (2024) e202302122, https://doi.org/10.1002/cbdv.202302122.
[29] J. Bouayed, H. Rammal, A. Dicko, C. Younos, R. Soulimani, Chlorogenic acid, a polyphenol from *Prunus domestica* (Mirabelle), with coupled anxiolytic and antioxidant effects, J. Neurol. Sci. 262 (2007) 77–84, https://doi.org/10.1016/j.jns.2007.06.028.
[30] K. Pei, J. Ou, J. Huang, S. Ou, p-Coumaric acid and its conjugates: dietary sources, pharmacokinetic properties and biological activities, J. Sci. Food Agric. 96 (2016) 2952–2962, https://doi.org/10.1002/jsfa.7578.
[31] L. Deng, X. Zhou, G. Tao, W. Hao, L. Wang, Z. Lan, Y. Song, M. Wu, J. Huang, Ferulic acid and feruloylated oligosaccharides alleviate anxiety and depression symptom via regulating gut microbiome and microbial metabolism, Food Res. Int. 162 (2022) 111887, https://doi.org/10.1016/j.foodres.2022.111887.
[32] M.H. Mahnashi, M. Ayaz, Y.S. Alqahtani, B.A. Alyami, M. Shahid, O. Alqahtani, S. M. Kabrah, A. Zeb, F. Ullah, A. Sadiq, Quantitative-HPLC-DAD polyphenols analysis, anxiolytic and cognition enhancing potentials of *Sorbaria tomentosa* Lindl. Rehder, J. Ethnopharmacol. 317 (2023) 116786, https://doi.org/10.1016/j.jep.2023.116786.
[33] A. Müller Herde, D. Benke, W.T. Ralvenius, L. Mu, R. Schibli, H.U. Zeilhofer, S. D. Krämer, GABAA receptor subtypes in the mouse brain: Regional mapping and diazepam receptor occupancy by in vivo [18F]flumazenil PET, NeuroImage 150 (2017) 279–291, https://doi.org/10.1016/j.neuroimage.2017.02.022.
[34] E.J.H. van van Hugte, D. Schubert, N. Nadif Kasri, Excitatory/inhibitory balance in epilepsies and neurodevelopmental disorders: Depolarizing γ-aminobutyric acid as a common mechanism, Epilepsia 64 (2023) 1975–1990, https://doi.org/10.1111/epi.17651.
[35] Z.M. Sheffler, V. Reddy, L.S. Pillarisetty, Physiology, Neurotransmitters, in: StatPearls, StatPearls Publishing, Treasure Island (FL), 2025. ⟨http://www.ncbi.nlm.nih.gov/books/NBK539894/⟩ (accessed January 23, 2026).
[36] N.C. Danbolt, Glutamate uptake, Prog. Neurobiol. 65 (2001) 1–105, https://doi.org/10.1016/S0301-0082(00)00067-8.
[37] A. Nugroho, M.-H. Kim, J. Choi, J.S. Choi, W.T. Jung, K.-T. Lee, H.-J. Park, Phytochemical studies of the phenolic substances in Aster glehni extract and its sedative and anticonvulsant activity, Arch. Pharm. Res. 35 (2012) 423–430, https://doi.org/10.1007/s12272-012-0304-7.
[38] F. Suciu, D.P. Mihai, A. Ungurianu, C. Andrei, C. Puşcaşu, C.L. Chițescu, R. V. Ancuceanu, C.E. Gird, E. Stefanescu, N.M. Blebea, V. Popovici, A.C. Rosca, C.I. V. Ghiță, S. Negres, Investigation of Anticonvulsant Potential of Morus alba, Angelica archangelica, Valeriana officinalis, and Passiflora incarnata Extracts: In Vivo and In Silico Studies, Int. J. Mol. Sci. 26 (2025), https://doi.org/10.3390/ijms26136426.
[39] D. Zheleva-Dimitrova, R. Gevrenova, M.M. Zaharieva, H. Najdenski, S. Ruseva, V. Lozanov, V. Balabanova, S. Yagi, G. Momekov, V. Mitev, HPLC-UV and LC–MS Analyses of Acylquinic Acids in Geigeria alata (DC) Oliv. & Hiern. and their Contribution to Antioxidant and Antimicrobial Capacity, Phytochem. Anal. 28 (2017) 176–184, https://doi.org/10.1002/pca.2658.
[40] D. Vauzour, G. Corona, J.P.E. Spencer, Caffeic acid, tyrosol and p-coumaric acid are potent inhibitors of 5-S-cysteinyl-dopamine induced neurotoxicity, Arch. Biochem. Biophys. 501 (2010) 106–111, https://doi.org/10.1016/j.abb.2010.03.016.
[41] H. Rommelspacher, C. Nanz, H.O. Borbe, K.J. Fehske, W.E. Müller, U. Wollert, Benzodiazepine antagonism by harmane and other β-carbolines in vitro and in vivo, Eur. J. Pharmacol. 70 (1981) 409–416, https://doi.org/10.1016/0014-2999(81)90173-4.
[42] W.E. Müller, K.J. Fehske, H.O. Borbe, U. Wollert, C. Nanz, H. Rommelspacher, On the neuropharmacology of Harmane and other β-carbolines, Pharmacol. Biochem. Behav. 14 (1981) 693–699, https://doi.org/10.1016/0091-3057(81)90133-7.
[43] F. Aricioglu, O. Yillar, E. Korcegez, K. Berkman, Effect of harmane on the convulsive threshold in epilepsy models in mice, Ann. N. Y. Acad. Sci. 1009 (2003) 190–195, https://doi.org/10.1196/annals.1304.023.
[44] U.P. Kundap, Y. Kumari, I. Othman, M.F. Shaikh, Zebrafish as a model for epilepsy-induced cognitive dysfunction: a pharmacological, biochemical and behavioral approach, Front. Pharmacol. 8 (2017), https://doi.org/10.3389/fphar.2017.00515.
[45] B.H.M. Mussulini, C.E. Leite, K.C. Zenki, L. Moro, S. Baggio, E.P. Rico, D. B. Rosemberg, R.D. Dias, T.M. Souza, M.E. Calcagnotto, M.M. Campos, A. M. Battastini, D.L. de Oliveira, Seizures Induced by Pentylenetetrazole in the Adult Zebrafish: a detailed behavioral characterization, PLOS ONE 8 (2013) e54515, https://doi.org/10.1371/journal.pone.0054515.
[46] W. Norton, L. Bally-Cuif, Adult zebrafish as a model organism for behavioural genetics, BMC Neurosci. 11 (2010) 90, https://doi.org/10.1186/1471-2202-11-90.
[47] D. Yusuf, A.M. Davis, G.J. Kleywegt, S. Schmitt, An Alternative Method for the Evaluation of Docking Performance: RSR vs RMSD, J. Chem. Inf. Model. 48 (2008) 1411–1422, https://doi.org/10.1021/ci800084x.
[48] Y. Wang, Y. Zhang, W. Li, B. Salovska, J. Zhang, T. Li, H. Li, Y. Liu, L.K. Kaczmarek, L. Pusztai, D.E. Klein, GABAA receptor π forms channels that stimulate ERK through a G-protein-dependent pathway, Mol. Cell. 85 (2025) 166–176.e5, https://doi.org/10.1016/j.molcel.2024.11.016.
[49] A. Maria Barros Alves, I.C. Romão, R. Jorge Souza, E. Silva Marinho, M. M. Marinho, M.N. Rocha, K.M. Canuto, J. Eire Silva Alencar Menezes, S. Maria Costa Siqueira, H.S. dos Santos, Synthesis, characterization, and evaluation of the anxiolytic activity of hydrazones derived from the drug isoniazid, using the adult zebrafish (Danio rerio) model, ACS Omega 10 (2025) 45152–45164, https://doi.org/10.1021/acsomega.5c04279.
[50] A. Imberty, K.D. Hardman, J.P. Carver, S. Perez, Molecular modelling of protein-carbohydrate interactions. Docking of monosaccharides in the binding site of concanavalin A, Glycobiology 1 (1991) 631–642, https://doi.org/10.1093/glycob/1.6.631.
[51] M. Naveed, V. Hejazi, M. Abbas, A.A. Kamboh, G.J. Khan, M. Shumzaid, F. Ahmad, D. Babazadeh, X. FangFang, F. Modarresi-Ghazani, L. WenHua, Z. XiaoHui, Chlorogenic acid (CGA): A pharmacological review and call for further research, Biomed. Pharmacother. 97 (2018) 67–74, https://doi.org/10.1016/j.biopha.2017.10.064.
[52] R. Santhanam, S. Ramesh, H.A.R. Suleria, Biology and Ecology of Pharmaceutical Marine Plants, CRC Press, Boca Raton, 2018, https://doi.org/10.1201/9781351187114.
[53] J. Bouayed, H. Rammal, A. Dicko, C. Younos, R. Soulimani, Chlorogenic acid, a polyphenol from *Prunus domestica* (Mirabelle), with coupled anxiolytic and antioxidant effects, J. Neurol. Sci. 262 (2007) 77–84, https://doi.org/10.1016/j.jns.2007.06.028.
[54] A.C.C.M. Castro, F.B. Oda, M.G.J. Almeida-Cincotto, M.G. Davanço, B.G. Chiari-Andréo, R.M.B. Cicarelli, R.G. Peccinini, G.J. Zocolo, P.R.V. Ribeiro, M.A. Corrêa, V.L.B. Isaac, A.G. Santos, Green coffee seed residue: a sustainable source of antioxidant compounds, Food Chem. 246 (2018) 48–57, https://doi.org/10.1016/j.foodchem.2017.10.153.
[55] A. Berger, E. Tanuhadi, L. Brecker, J. Schinnerl, K. Valant-Vetschera, Chemodiversity of tryptamine-derived alkaloids in six Costa Rican Palicourea species (Rubiaceae–Palicoureeae), Phytochemistry 143 (2017) 124–131, https://doi.org/10.1016/j.phytochem.2017.07.016.